THE GEOLOGICAL SOCIETY OF AMERICA®

Trough geometry was a greater influence than climate-ocean forcing in regulating retreat of the marine-based Irish-Sea Ice Stream

David Small[1,2,†], Rachel K. Smedley[3,4], Richard C. Chiverrell[4], James D. Scourse[5], Colm Ó Cofaigh[2], Geoff A.T. Duller[3], Stephen McCarron[6], Matthew J. Burke[4], David J.A. Evans[2], Derek Fabel[7], Delia M. Gheorghiu[8], Geoff S.P. Thomas[4], Sheng Xu[8], and Chris D. Clark[9]

[1]*School of Geographical and Earth Sciences, University of Glasgow, Glasgow, UK*
[2]*Department of Geography, Durham University, Durham, UK*
[3]*Department of Geography and Earth Sciences, Aberystwyth University, Ceredigion, UK*
[4]*School of Environmental Sciences, University of Liverpool, Liverpool, UK*
[5]*Centre for Geography, Environment and Society (CGES), College of Life and Environmental Sciences, University of Exeter, Penryn Campus, Penryn, Cornwall, UK*
[6]*Department of Geography, Maynooth University, Maynooth, Ireland*
[7]*Scottish Universities Environmental Research Centre, East Kilbride, UK*
[8]*Natural Environment Research Council (NERC), Cosmogenic Isotope Analysis Facility-Scottish Universities Environmental Research Centre (CIAF-SUERC), East Kilbride, UK*
[9]*Department of Geography, University of Sheffield, Sheffield, UK*

ABSTRACT

Marine terminating ice streams are a major component of contemporary ice sheets and are likely to have a fundamental influence on their future evolution and concomitant contribution to sea-level rise. To accurately predict this evolution requires that modern day observations can be placed into a longer-term context and that numerical ice sheet models used for making predictions are validated against known evolution of former ice masses. New geochronological data document a stepped retreat of the paleo–Irish Sea Ice Stream from its Last Glacial Maximum limits, constraining changes in the time-averaged retreat rates between well-defined ice marginal positions. The timing and pace of this retreat is compatible with the sediment-landform record and suggests that ice marginal retreat was primarily conditioned by trough geometry and that its pacing was independent of ocean-climate forcing. We present and integrate new luminescence and cosmogenic exposure ages in a spatial Bayesian sequence model for a north-south (173km) transect of the largest marine-terminating ice stream draining the last British–Irish Ice Sheet. From the south and east coasts of Ireland, initial rates of ice margin retreat were as high as 300–600 m a^{-1}, but retreat slowed to 26 m a^{-1} as the ice stream became topographically constricted within St George's Channel, a sea channel between Ireland to the west and Great Britain to the east, and then stabilized (retreating at only 3 m a^{-1}) at the narrowest point of the trough during the climatic warming of Greenland Interstadial 2 (GI-2: 23.3–22.9 ka). Later retreat across a normal bed-slope during the cooler conditions of Greenland Stadial 2 was unexpectedly rapid (152 m a^{-1}). We demonstrate that trough geometry had a profound influence on ice margin retreat and suggest that the final rapid retreat was conditioned by ice sheet drawdown (dynamic thinning) during stabilization at the trough constriction, which was exacerbated by increased calving due to warmer ocean waters during GI-2.

INTRODUCTION

A significant proportion of ice sheet mass balance is regulated by faster flowing corridors of ice (ice streams), which drain accumulation areas and are often marine-terminating (Stokes and Clark, 2001; Bennett, 2003; Stokes et al., 2016). While climate forcing exerts a fundamental control on the retreat of ice masses, internal factors such as phases of over-extension (i.e., an advance due to a dynamic instability rather than toward an equilibrium position), the bed-slope and trough geometry are also important regulators of ice stream behavior (Jamieson et al., 2012; Joughin et al., 2014; Mosola and Anderson, 2006). Marine-terminating ice streams are also susceptible to oceanic influence, including changes in relative sea level, sea surface temperatures and tidal regime (Payne et al., 2004; Arbic et al., 2008). There is presently substantial concern about anthropogenically forced atmospheric and oceanic warming causing the rapid retreat of marine-terminating ice streams in Greenland and Antarctica (Joughin and Alley, 2011; Rignot et al., 2014). To understand fully and predict how these ice masses will evolve, there is a need to understand the complex interactions between external forcings and internal dynamics in modulating ice marginal retreat (e.g., Benn et al., 2007; Jamieson et al., 2012; Schoof, 2007). Constraining the evolution of former ice streams provides important empirical evidence for testing process understanding of modern-day ice masses and evaluating numerical ice sheet models (Stokes et al., 2015).

The Irish Sea Ice Stream (ISIS; Fig. 1) was the largest marine-terminating ice stream to drain the former British–Irish Ice Sheet (BIIS) (Eyles and McCabe, 1989) and during deglaciation it formed an example of marine-based ice stream retreat. The sediments and landforms along the southern and eastern coastal lowlands of Ireland, with >30 km extent of intermittent coastal exposure between the south coast and Dublin (~170 km; Fig. 1), record the dynamics of the western lateral margin of the paleo–ISIS during the last deglaciation. We propose a conceptual model for the retreat of the ISIS inferred from the sediment-landform assemblages and constrain this using a new data set of 13 opti-

†david.p.small@durham.ac.uk

GSA Bulletin; November/December 2018; v. 130; no. 11/12; p. 1981–1999; https://doi.org/10.1130/B31852.1; 13 figures; 6 tables; Data Repository item 2018183; published online 28 May 2018.

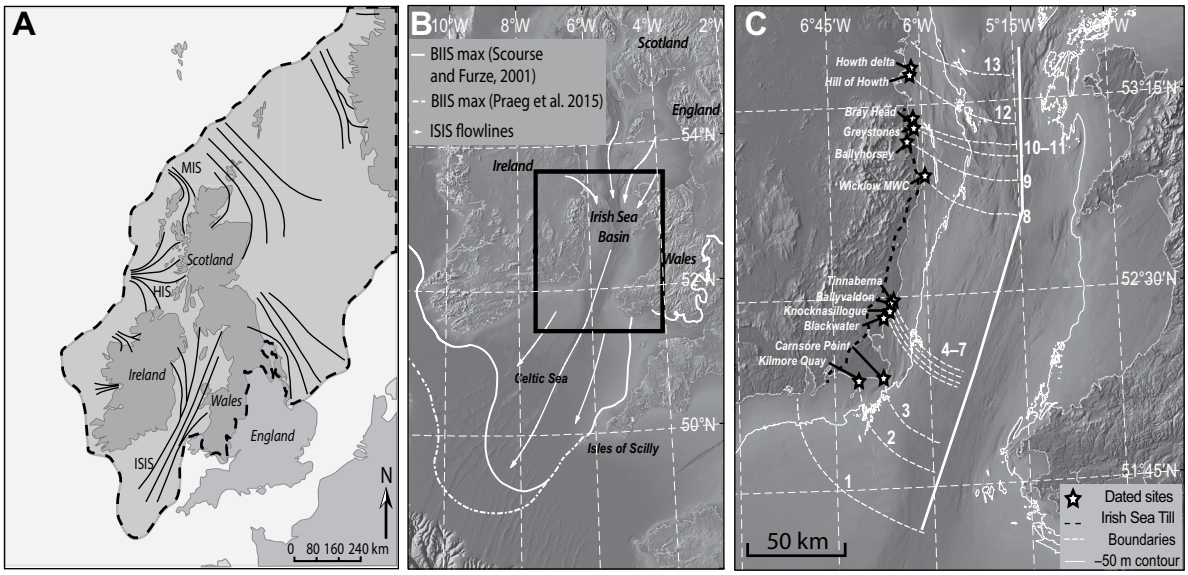

Figure 1. (A and B) Location map of study area within former British–Irish Ice Sheet (BIIS) and (A) a close up of its relative position with respect to the southern portion of the former BIIS. (C) Study area with solid white line indicating trough axis used to calculate axial retreat distances. Dashed white lines are boundaries defined in Bayesian sequence model, numbered as in Figure 2 and Table 5. Note Boundary 9 is constrained by samples from altitude, hence its location within the sequence. Sample locations are shown with white stars and site names are as Tables 1 and 5. The thick black line denotes the limit of till-bearing accessory erratics indicative of an Irish Sea provenance. MIS—Minch Ice Stream; HIS—Hebrides Ice Stream; ISIS—Irish Sea Ice Stream; MWC—meltwater channel.

cally stimulated luminescence (OSL) and 10 cosmogenic nuclide (CN) exposure ages. OSL dating was applied to glacial sediments (glacial outwash) that can be correlated with the presence of a proximal ice margin. CN dating was applied to glacially transported boulders and bedrock to directly constrain the timing of ice margin retreat. The new chronological data are integrated using a Bayesian sequence model and the pace of ice-marginal retreat is compared with existing data sets to explore the importance of potential driving factors. These factors include North Atlantic oceanic and climatic forcing, changes in the confining geometry of the ISIS in the southern Irish Sea Basin (ISB) (e.g., bed-slope and trough geometry) and the feedbacks in the sequence of ice flow behavior with potential over-extension identified in a rapid advance of the ISIS to maximum limits (Chiverrell et al., 2013; Ó Cofaigh and Evans, 2007; Smedley et al., 2017a).

THE IRISH SEA ICE STREAM

The last ISIS (Fig. 1: Eyles and McCabe, 1989) drained on-shore ice accumulation areas in Ireland, northern England, and southern Scotland (cf. Roberts et al., 2007) and at its maximum extent ca. 25 ka (Ó Cofaigh and Evans, 2007; Smedley et al., 2017a) extended into the Celtic Sea (Scourse et al., 1990; Scourse and Furze, 2001; Hiemstra et al., 2006), possibly as far as the shelf break (Praeg et al., 2015). The advance to this maximum limit has been hypothesized as a rapid, and perhaps short lived, surge-type event (Scourse and Furze, 2001; Ó Cofaigh and Evans, 2001a, 2001b, 2007). Coastal exposures of glacigenic sediments show ubiquitous diamictons containing erratic clasts of an Irish Sea affinity (Irish Sea Tills: Ó Cofaigh and Evans, 2001a, 2001b) and document on-shore flow of ice (Thomas and Summers, 1983; Ó Cofaigh and Evans, 2001b, 2007; Evans and Ó Cofaigh, 2003). These sediments have been interpreted as representing: (1) the deglacial transition from subglacial to proximal and then distal glacimarine sedimentation in an isostatically-depressed ISB (Eyles and McCabe, 1989; Clark et al., 2012; McCabe, 1997), or (2) subglacial and ice marginal deposition at the lateral grounded margin of an ice stream (Thomas and Summers, 1983, 1984; Ó Cofaigh and Evans, 2001a, 2001b; Evans and Ó Cofaigh, 2003). The glacimarine hypothesis is considered unlikely given the magnitude of isostatic loading required (cf. Lambeck and Purcell, 2001; Bradley et al., 2011) and the lack of unambiguous evidence for glacimarine sedimentation (Ó Cofaigh and Evans, 2001a; Evans and Ó Cofaigh, 2003; Rijsdijk et al., 2010). The sediment-landform assemblages distributed along the southern and eastern coasts of Ireland provide the evidence base for a conceptual model for the relative order of retreat events and suggests that the ISIS experienced marked changes in the rate of retreat (Fig. 2).

Rapid Initial Advance and Retreat

Initial advance of the ISIS is recorded along the south Irish coast by subglacial diamictons with erratics of Irish Sea provenance (Ó Cofaigh and Evans, 2001a, b). These diamictons contain abundant reworked marine fauna and the youngest ages from a population of 26 radiocarbon ages indicate that advance occurred after ca. 25–24 ka (Ó Cofaigh and Evans, 2007). The timing of the maximum extent of the ISIS on the Isles of Scilly, UK, is indistinguishable within dating uncertainties with new OSL and CN ages constraining this to 25.5 ± 1.5 ka (Smedley et al., 2017a). The Irish Sea diamictons exposed along the south coast of Ireland are overlain by glacial outwash and localized glacilacustrine deposits that record proglacial deposition along the retreating margin of the ISIS (Fig. 3; Ó Cofaigh and Evans, 2001a, 2001b). Finally, following retreat of the ISIS, ice sourced in the Irish midlands advanced beyond the present-day coastline depositing glacial till that is rich in lithologies of an inland origin and deforming the underlying glacifluvial and glacilacustrine sequence (Ó Cofaigh and Evans, 2001a, 2001b).

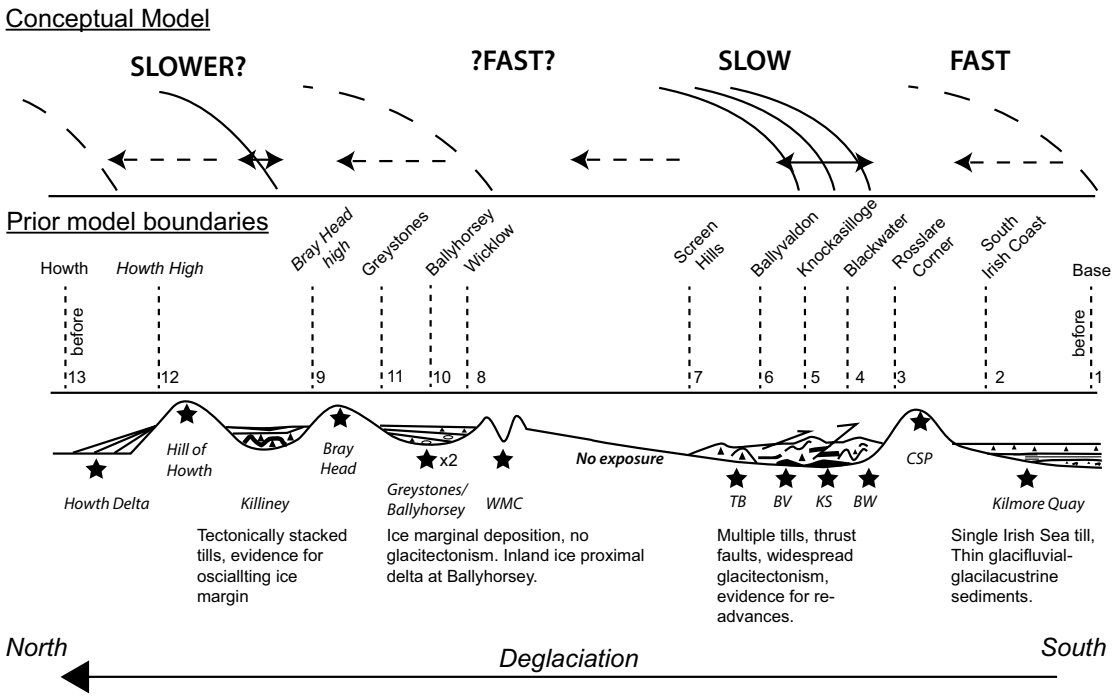

Figure 2. Conceptual model of sequence and rates of Irish Sea Ice Stream (ISIS) deglaciation based on existing geomorphological and sedimentary studies. Boundary numbers and names (cf Fig. 1 and Table 5) are shown in the center panel. Sample sites and names are denoted by stars in the lower panel. Note that the sample locations at Ballyhorsey, Greystones, and Bray Head, Ireland, are in close proximity, but are separated by >200 m elevation. For deglaciation to have occurred at these sites simultaneously would require a glacier gradient that is physically unlikely. Consequently, we consider it likely that Bray Head was deglaciated prior to Greystones and Ballyhorsey and order them accordingly in our prior model. CSP—Carnsore Point, BW—Blackwater, KS—Knocknasillogue, BV—Ballyvaldon, TB—Tinnaberna, WMC—Wicklow meltwater channel.

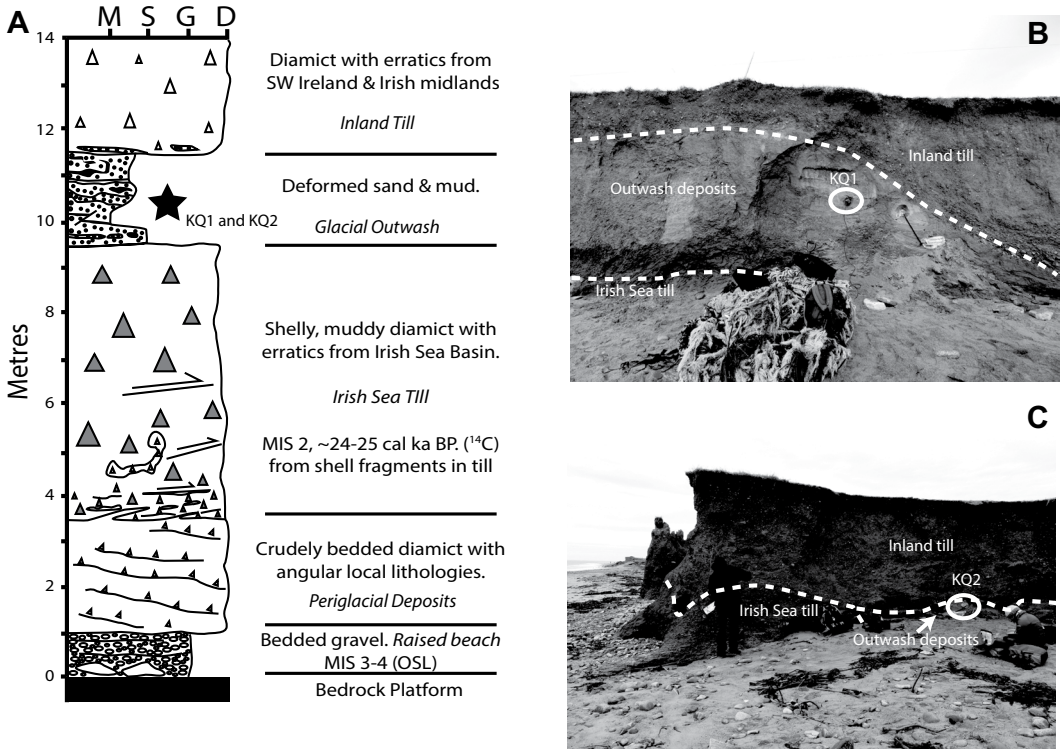

Figure 3. (A) Composite stratigraphic log of the south coast sequence at Kilmore Quay, Co. Wexford, Ireland, (from Ó Cofaigh and Evans, 2007) showing Irish Sea Till overlying periglacial slope deposits and a raised beach and overlain by glacilacustrine and glacifluvial outwash deposits and a till of inland origin. The location of the optically stimulated luminescence (OSL) samples KQ1 and KQ2 within this sequence is shown. MIS—marine isotope stage; M—Mud; S—Sand; G—Gravel; D—Diamict. (B and C) Shows sample locations of dated OSL samples KQ1 and KQ2.

The thin and discontinuous nature of these deposits perhaps reflects a relatively rapid retreat with limited development of ice-marginal landforms. This inference is supported by an earlier Bayesian model using legacy geochronological data that suggests that ISIS advance to—and retreat from—its maximum limit was rapid (<1 ka) (Chiverrell et al., 2013).

Establishment of an Oscillating Grounded Ice Margin

Sediment-landform assemblages related to the ISIS also crop out along the east coast of Ireland and provide evidence for relatively greater complexity in ice marginal dynamics. The Screen Hills (Fig. 4) represent the largest glacigenic sedimentary depocenter on the east coast of Ireland, with >150 km^2 of glacial landforms and ~20 km of coastal exposures that locally reach >50 m in height. The stratigraphy reflects the interaction of subglacial processes and ice marginal deposition, including thrusting and stacking of glacigenic units, and results from at least eleven minor (< km scale) readvances of the ISIS margin (Evans and Ó Cofaigh, 2003; Thomas and Chiverrell, 2011; Thomas and Summers, 1984, 1983). The sequence suggests that ice marginal retreat slowed as the ISIS margin retreated from the Celtic Sea into St George's Channel (cf. Evans and Ó Cofaigh, 2003) and that a dynamic and oscillating margin was established (Thomas and Summers, 1983, 1984; Thomas and Kerr, 1987; Evans and Ó Cofaigh, 2003).

Renewed Rapid Ice Marginal Retreat?

Further north exposures of glacial sediments related to the ISIS are more sporadic (Fig. 1), which might reflect more rapid ISIS retreat, but extensive Holocene sand dunes may mask the glacial sequence locally. There are no sediment exposures or geomorphological features indicative of ice margin oscillations or any large scale readvance(s) north of the Screen Hills. Consequently, it is inferred that retreat from the Screen Hills was a quasi-continuous process. The first ice marginal position north of the Screen Hills occurs at Greystones, Co. Wicklow, Ireland, which has been interpreted as a morainal bank complex deposited in an ice proximal subaqueous basin prograding from a bedrock high (McCabe, 2008). The sections display no evidence for oscillation or readvance of the ice margin (McCabe and Ó Cofaigh, 1995). Further north at Killiney, Co. Dublin, Ireland, glacial diamictons (Irish Sea and inland origin) and outwash deposits form a complex sequence of glacitectonically stacked units resulting from overriding by ice and oscillation of the ice margin during ISIS retreat (Rijsdijk et al., 2010).

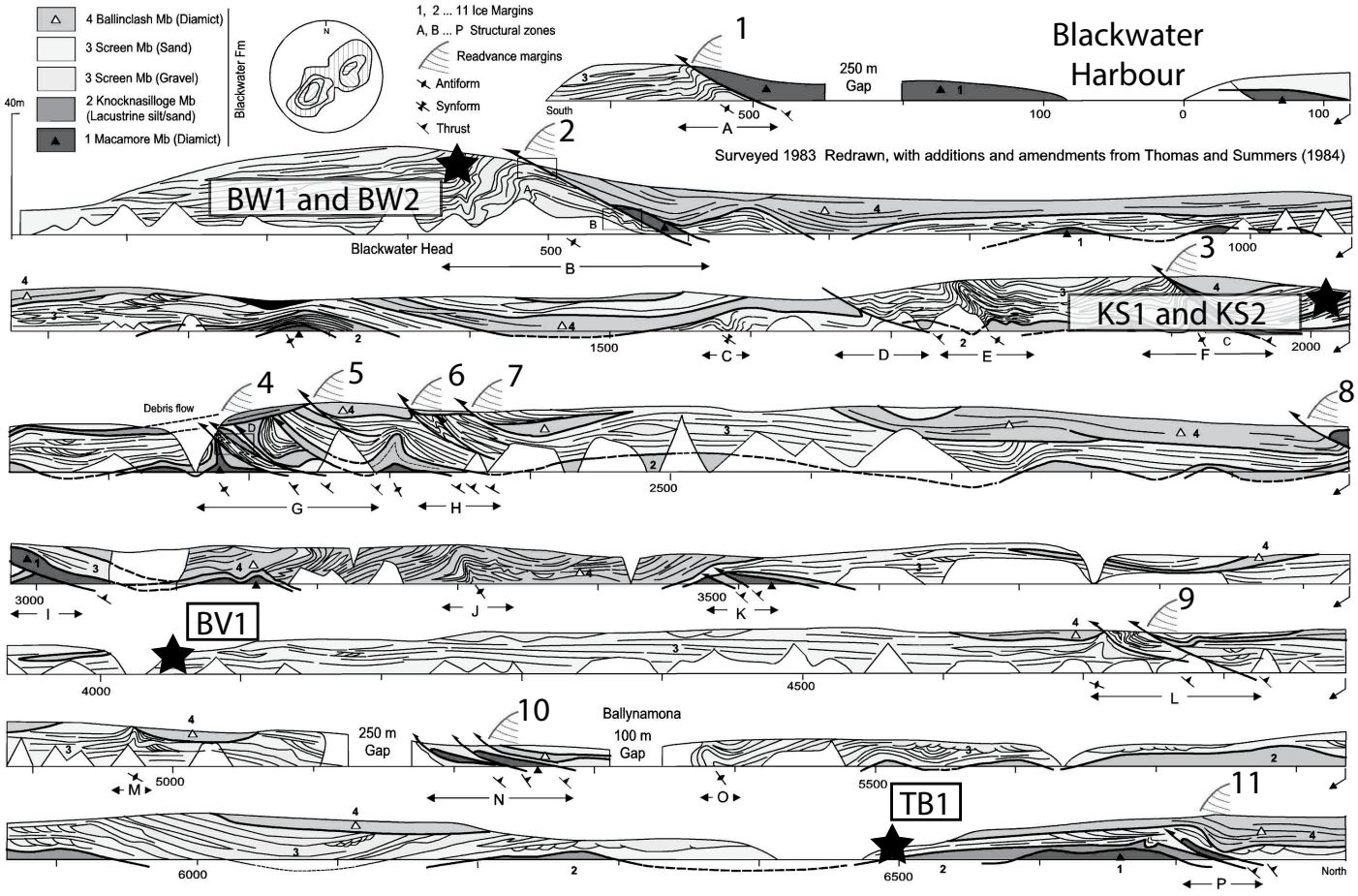

Figure 4. The stratigraphy of the Screen Hills sequence between Blackwater Harbour and Tinnaberna, Co. Wexford, Ireland, showing zones of glacitectonic deformation (A–P) and readvance limits (1–11). Length of section is ~7 km. Inset at top shows stereogram (Wulff, lower hemisphere) of 278 measurements of poles to thrust planes and fold limbs. Contours at 1, 3, 5, and 10%. Locations of optically stimulated luminescence samples within this sequence are shown. Redrawn from Thomas and Chiverrell (2011) with additions from Thomas and Summers (1983, 1984).

FIELD SITES

The conceptual model (Fig. 2) for ISIS retreat informed our field sampling strategy with sites distributed to provide geochronological constraints on the timing and pace of deglaciation throughout the region. The 14 OSL samples from eight sites targeted glacial outwash sands associated primarily with known ice marginal positions and locations (Table 1) through the retreat sequence. The CN dating using in situ ^{10}Be targeted a mixture of glacially modified bedrock outcrops or glacially faceted and transported boulders producing 10 samples from four locations (Table 2).

TABLE 1. LOCATION INFORMATION OF ALL OSL SAMPLES

BRITICE-CHRONO sample code	Short sample code	Site	Lat (°N)	Long (°E)	Elevation (m ASL)
T4KQUY01	KQ1	Kilmore Quay	52.179	–6.5597	2
T4KQUY02	KQ2	Kilmore Quay	52.1812	–6.5549	2
T4WEXF1A	BW1	Blackwater	52.4316	–6.3263	11
T4WEXF1B	BW2	Blackwater	52.4316	–6.3263	12.5
T4WEXF2A	KS1	Knocknasillogue	52.4451	–6.3128	20
T4WEXF2B	KS2	Knocknasillogue	52.4451	–6.3128	20.7
T4WEXF03	BV1	Ballyvaldon	52.4642	–6.2948	8
T4WEXF4A	TB1	Tinnaberna	52.4813	–6.274	10
T4WEXF4B	TB2	Tinnaberna	52.4813	–6.274	5
T4BHOR01	BH1	Ballyhorsey	53.1059	–6.2948	10
T4BHOR02	BH2	Ballyhorsey	53.1059	–6.2948	10.5
T4GREY01	GY1	Greystones	53.165	–6.0767	12.5
T4HOWT01	HD1	Howth Delta	53.3867	–6.0642	10
T4HOWT02	HD2	Howth Delta	53.3867	–6.0642	11.5

Note: All sites are located in SE Ireland. OSL—optically stimulated luminescence; ASL—above sea level.

Kilmore Quay

The exposures at Kilmore Quay, Co. Wexford, Ireland, have previously been described in detail (Ó Cofaigh and Evans, 2001a; Evans and Ó Cofaigh, 2003). Two samples were taken from the coastal cliff where relatively thin glacifluvial sands overlie Irish Sea tills that crop out at the base of the sequence. KQ1 and KQ2 were collected for OSL dating from medium- to fine-sand units (Fig. 3; Table 2) to constrain the timing of ISIS marginal retreat onto the south coast of Ireland. While the sequences are generally glacitectonised the sands retain primary depositional features such as ripples.

Carnsore Point

Twelve km east of Kilmore Quay, Carnsore Point, Co. Wexford, Ireland, is characterized by a spread of large granite boulders derived from local outcrop of the Carnsore Granite (O'Connor et al., 1988). The boulders occur on the surface and reflect deposition by the retreating ISIS given the lack of sedimentary evidence for readvances of inland ice in this area (Evans and Ó Cofaigh, 2003). There is no obvious orientation to the spread of boulders and no other glacial landforms in the immediate vicinity. Many boulders exhibit signs of human activity including incorporation into field boundaries (Fig. 5A and Fig. DR6 in GSA Data Repository[1]). Some of these however, were inferred in the field to be in situ and three samples (CS1–3) were collected for analysis with ^{10}Be to provide constraint on the passage of the ice margin from the south coast of Ireland into St George's Channel.

Screen Hills

Thirty km to the northeast of Carnsore Point, the Screen Hills represent the largest accumulation of glacial sediments on the east coast of Ireland (Evans and Ó Cofaigh, 2003; Thomas and Chiverrell, 2011; Thomas and Summers, 1983, 1984). OSL samples were collected from glacifluvial outwash sands at four sites which were chosen from the ~15 km of continuous coastal exposure studied in detail by Thomas and Summers (1983, 1984) extending from Blackwater Harbour in the south to Tinnaberna in the north, Co. Wexford, Ireland (Fig. 4). These relate to well-defined ice marginal positions (Thomas and Summers, 1984; Thomas and Chiverrell, 2011) and the sampled units retain primary depositional features such as ripples and faint laminations. Progressing from south to north—near Blackwater Harbour—two samples of medium–coarse sands with faint ripples (BW1) and laminations (BW2) were collected from a >30-m-thick wedge of outwash sands and gravels that thin to the south away from a glacitectonised ice marginal position (Limit 2: Fig. 4; Thomas and Chiverrell, 2011). The samples were collected at 5–8 m depth in the 20-m-thick series of alternating outwash sand and gravel sheets that dip gently to the south and overlie a basal diamicton (Fig. 6A). Knocknasillogue, Co. Wexford, Ireland, is ~1.7 km further to the northeast, and two samples separated vertically by ~1 m (KS1 and

[1]GSA Data Repository item 2018183, details on optically stimulated luminescence methodology and background information on sites, is available at http://www.geosociety.org/datarepository/2018 or by request to editing@geosociety.org.

TABLE 2. SAMPLE INFORMATION, CHEMISTRY DATA AND MEASURED ^{10}BE/^{9}BE RATIOS FOR CN SAMPLES

BRITICE-CHRONO sample code	Short sample code	Lat (°N)	Long (°E)	Alt. (m ASL)	Thickness (cm)	Shielding correction*	Boulder dimensions (m)	Qtz Mass (g)	Be Spike† (µg)	^{10}Be/^{9}Be §,#	Uncert.
T4CSP01	CS1	52.1795	–6.3749	10	3	1	1.5 × 1.3 × 1.1	21.48	253.77	** 6.19×10^{-14}	1.95×10^{-15}
T4CSP02	CS2	52.1808	–6.3739	10	4	1	2.8 × 2.2 × 1.5	21.87	253.94	** 1.43×10^{-13}	3.49×10^{-15}
T4CSP03	CS3	52.1848	–6.3920	14	2	1	1.8 × 1.2 × 1.0	21.47	249.18	†† 1.25×10^{-13}	3.46×10^{-15}
T4WIK01	WK1	52.9722	–6.0093	13	3	0.826	N/A	21.69	254.28	** 8.73×10^{-13}	2.61×10^{-15}
T4WIK02	WK2	52.9722	–6.0093	13	3	0.824	N/A	20.27	220.32	## 1.06×10^{-13}	2.96×10^{-15}
T4BRY01	BR1	53.1806	–6.0800	215	2	1	1.4 × 1.1 × 1.0	16.81	247.91	†† 1.03×10^{-13}	3.04×10^{-15}
T4BRY02	BR2	53.1791	–6.0811	221	3	1	N/A	20.04	224.14	## 1.58×10^{-13}	5.44×10^{-15}
T4BRY03	BR3	53.1791	–6.0811	221	2	0.994	N/A	20.02	222.44	## 1.47×10^{-13}	4.21×10^{-15}
T4HOH01	HO1	53.3734	–6.0967	171	2	1	N/A	16.13	221.25	## 1.36×10^{-13}	3.85×10^{-15}
T4HOH02	HO2	53.3734	–6.0967	171	3	1	N/A	20.12	214.80	## 1.44×10^{-13}	5.27×10^{-15}

Note: CN—cosmogenic nuclide; ASL—above sea level; Qtz—quartz.
*Topographic shielding correction calculated using online calculator (Balco et al., 2008; available at http://hess.ess.washington.edu/math/general/skyline_input.php).
†Samples were spiked with ^{9}Be carrier 849 ± 12 µg/g.
§Relative to NIST_27900 with ^{10}Be/^{9}Be taken as 2.79×10^{-11}.
#Ratios not blank corrected.
**Corrected for a process blank with ^{10}Be/^{9}Be ratio of $4.85 \pm 0.61 \times 10^{-15}$.
††Corrected for a process blank with ^{10}Be/^{9}Be ratio of $2.37 \pm 0.41 \times 10^{-15}$.
##Corrected for a process blank with ^{10}Be/^{9}Be ratio of $6.05 \pm 0.84 \times 10^{-15}$.

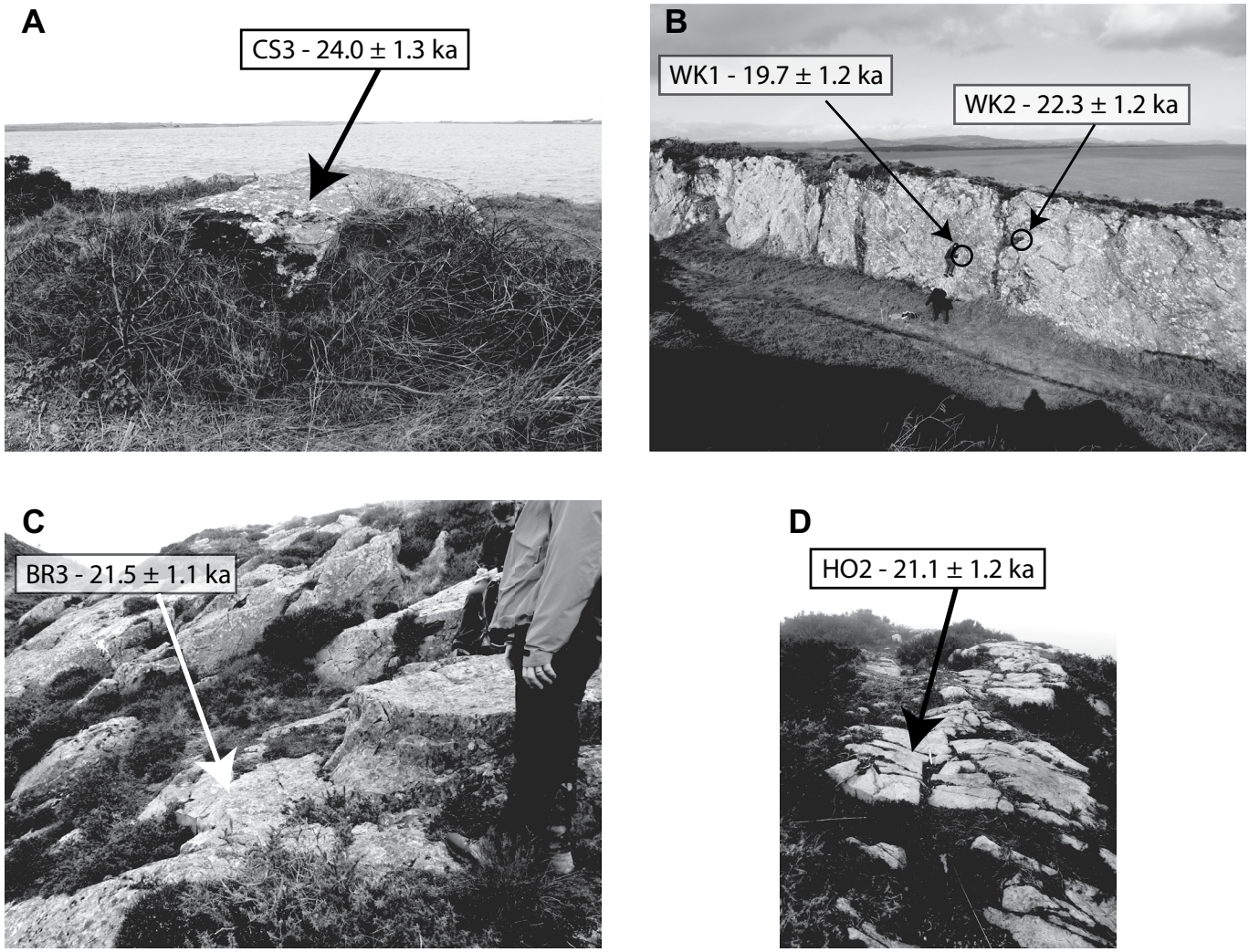

Figure 5. Photographs of selected cosmogenic nuclide (CN) samples discussed in the text. (A) Boulder incorporated at Carnsore point, Co. Wexford, Ireland. (B) Wicklow meltwater channel showing the location of samples collected. (C) Plucked lee slope on Bray Head, Co. Wicklow, Ireland, sampled for CN dating (ice flow right to left). (D) Glacially abraded surface on summit of Hill of Howth, Co. Dublin, Ireland. Striations and small scale p-forms are preserved (ice flow toward camera). Location of sample HH2 is shown. HH1 was collected from a similar outcrop of abraded quartzite bedrock.

KS2) were collected from a depth of ~10 m in medium-fine rippled sands with fine laminations (Fig. 6B). The sampled sequence is immediately up-ice of a pronounced glacitectonised marginal position (Limit 3: Fig. 4; Thomas and Chiverrell 2011). The sampling targeted the upper portion of a ~20-m-thick sequence of sands and gravels that overlie a basal Irish Sea diamicton, with both units thrust forward and upwards in a glacitectonic episode linked to the capping diamicton that completes the vertical succession. At Ballyvaldon, Co. Wexford, Ireland, ~2.3 km to the northeast, a single sample (BV1) of medium-coarse sands was collected at 10 m depth from a ~20 m thick and laterally extensive sequence of outwash sands fronting an ice marginal position ~700 m to the north (Limit 9: Fig. 4; Fig. 6C; Thomas and Chiverrell, 2011). At Tinnaberna, a further ~2.4 km to the northeast, two samples (TB1 and TB2) were collected from sand layers within alternating outwash sands and gravels fronting a further glacitectonised ice marginal positions (Limit 11: Fig. 4; Thomas and Chiverrell, 2011). The samples were taken from outwash sands ~4 m to 0.5 m above a basal Irish Sea diamicton at burial depths of 10 m and 20 m, respectively, but TB2 did not yield an age determination.

Wicklow Point

Fifty km north of Tinnaberna, there is a distinct channel orientated E–W and cut into schist bedrock at ~15 m above sea level (ASL) on Wicklow Point (Fig. 5B and Fig. DR6 in GSA Data Repository). The channel is ~250 m long and 10 m wide, widening to 20 m at its southern end and has an undulating thalweg. The onset and end of the channel are abrupt and there is no catchment, a configuration common in subglacial meltwater channels. The feature is therefore interpreted as a likely subglacial meltwater channel. The channel would have been exposed during deglaciation and thus two samples were collected for ^{10}Be analysis from the channel wall, >3 m from the top of the channel (WK1-2). This site was chosen to provide constraints on deglaciation between the sedimentary exposures at the Screen Hills and Greystones.

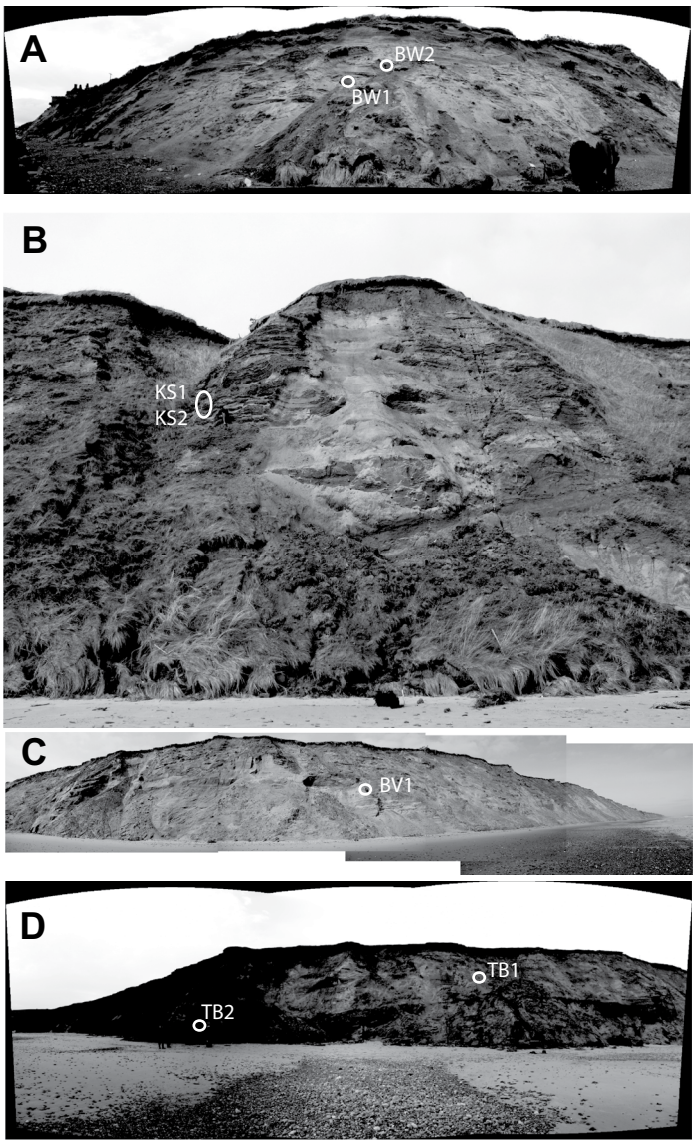

Figure 6. Sections sampled for optically stimulated luminescence (OSL) dating within the Screen Hills complex, near the southeast coast of Ireland. (A) Blackwater, (B) Knocknasillogue, (C) Ballyvaldon, and (D) Tinnaberna. Locations of OSL samples are shown alongside sample codes.

Ballyhorsey Quarry

Located 5 km inland from coastal sections lies a series of low-level (<120 m ASL) basins separated by bedrock-cored ridges. Drainage channels fret these bedrock ridges (Ravier et al., 2014), and they locally feed substantial proglacial depocenters (see Fig. DR7 in GSA Data Repository [footnote 1]). At Ballyhorsey a former sand and gravel quarry has provided exposures into extensive sub- and proglacial outwash in the "Kilpedder Basin" as described by Ravier et al. (2014) (Fig. 7). The lower sections studied by these authors document basal diamictons that interdigitate with glacifluvial deposits that formed subglacially. These units are buried by prograding subaqueous glacilacustrine fan facies that prograde and dip southwards as wedges and both thin and fine (from gravels to sands) with increasing distance from the ice-contact fan apex. This fan was likely deposited in a lake dammed by Irish Sea ice situated to the north and east (Ravier et al., 2014). In March 2014, the exposures were much degraded, but reasonable exposures were identified at the top of the sequence in the northwest corner of the quarry. These exposures were within 2–3 m of a flat horizontal surface and displayed horizontally and planar bedded and rippled fine to medium sands that we interpret as deltaic top-sets formed during the late stages of deposition. Two samples (BH1 and BH2) were collected from fine–medium planar sands with ripples preserved from the uppermost ice proximal delta top-set sands (Fig. 7).

Greystones

On the coast ~22 km north of Wicklow Point and ~7 km northeast of the Ballyhorsey Quarry, extensive (1.7 km) cliff exposures at Greystones document a substantial ice marginal position (Fig. 1). McCabe and Ó Cofaigh (1995) interpreted the sequence as morainal bank deposits that accumulated in a subaqueous setting by subglacial discharge from the ice margin, with the sequence deposited so that it did not evolve into a Gilbert-type delta. In March 2014, the exposures showed thin (2–3 m thickness) sand and gravel delta foresets (Fig. 8) with associated horizontally bedded sands and gravels interpreted as thin topsets. A single sample (GR1) was taken from this thin (~1 m) rippled sand unit that lies above 10–15 m of subaqueous outwash gravels and diamictons of Irish Sea provenance. Relating the unit sampled to the descriptions of McCabe and Ó Cofaigh (1995), it appears to correlate with a thin (>1 m) horizontally stratified series of ripped sands (Sr) interbedded with planar gravels (Gms) that lie immediately below their uppermost lithofacies (LFA4) which comprised 3.5 m of planar massive and poorly sorted gravels (Gm and Gms).

Bray Head

Five km north of the Greystones site, Bray Head is a hill (240 m ASL) composed of quartzite bedrock that shows extensive signs of glacial modification. Abraded and striated surfaces are present on the summit ridge of Bray Head with striations orientated in a general NNW-SSE direction. Plucked faces also occur on the lee side of flow. A single granite erratic boulder was located on Bray Head, ~250 m north of the summit. Given its altitude and proximity to the Greystones site, Bray Head may have been deglaciated prior to deposition of the sediments from which the optically stimulated luminescence (OSL) sample GR1 was taken. In addition to the granite erratic (BR1), two bedrock samples were collected from 220 m ASL on the summit ridge of Bray Head; one sample was collected from an abraded surface (BR2) with a further sample taken from a plucked surface (BR3) that lay >2.5 m beneath the upper abraded surface (Fig. 5C and Fig. DR6 in GSA Data Repository).

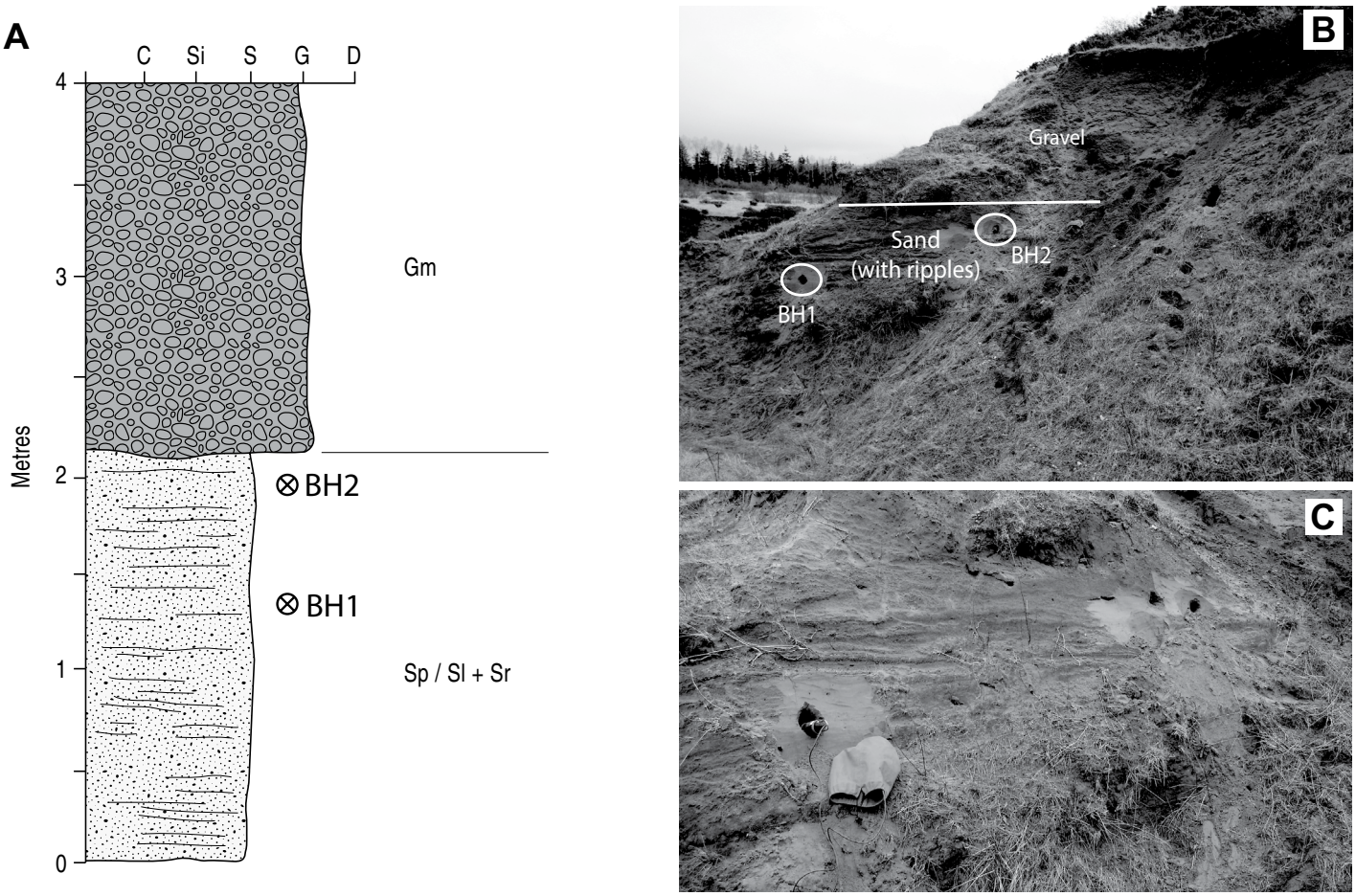

Figure 7. (A) Stratigraphic log of sampled section within Ballyhorsey Quarry, Co. Wicklow, Ireland, with optically stimulated luminescence sample locations indicated. (B) Photographs of sampled section showing sample context. (C) A close up of sampled unit.

Howth Peninsula

Howth is a peninsula 4 km in length that forms the north coast of Dublin Bay, Co. Dublin, Ireland. The Hill of Howth (171 m ASL) lies in the center of the peninsula and is composed primarily of quartzite. At its summit there is clear evidence of glacial abrasion (Fig. 5D and Fig. DR8 in GSA Data Repository). Striae indicate ice-movement from the north (Stephens and Synge, 1957) as the ISIS impinged onto the eastern coast of Ireland. Two samples were collected from the summit of the Hill of Howth from abraded quartzite bedrock (HH1–2). On the north side of the peninsula there is a ~0.5 km^2 deposit of stratified sands and gravels (Fig. 9) extending inland that has a maximum thickness of ~15 m (Lamplugh, 1903). The deposits have been interpreted as deltaic in origin composed mainly of reworked glacial deposits transported along local drainage lines and deposited in an ice marginal water-body (Lamplugh, 1903). The sequence was deposited after retreat of the ice margin north and west of Howth but while the ISIS was still present in the ISB to the east and ponding ice-dammed meltwater in Dublin Bay. Two OSL samples (HD1–2) were taken from fine–medium rippled sands that represent the topsets of the "Howth Delta."

METHODS

OSL Dating

Samples for OSL dating were collected by hammering opaque tubes into the sedimentary sections. External gamma dose-rates were determined in situ using field gamma spectrometry. Concentrations of U, Th, K, and Rb were determined for each sample using inductively coupled plasma–mass spectrometry (ICP-MS) and atomic emission spectroscopy (ICP-AES) (Table 3). These concentrations were used to calculate the external beta dose-rates and in situ gamma spectrometry determined the external gamma dose-rate. Sample preparation and analysis followed methods outlined in Smedley et al. (2017a). Single grains of quartz were used to determine equivalent dose (D_e) values (Tables DR1–DR14; Figs. DR1–DR3 in GSA Data Repository [footnote 1]) using a Risø TL/OSL DA-15 automated single-grain system equipped with a $^{90}Sr/^{90}Y$ beta source (Bøtter-Jensen et al., 2003). Grain sizes of 210–250 μm were used for OSL analysis of each sample, except sample KQ1 that had a grain size 150–180 μm and so it was likely that up to four grains were present in each hole on the single-grain disc (i.e., micro-hole measurements). Sample analysis methods are summarized in the GSA Data Repository (see footnote 1). The D_e distribution of sample TB2 (Fig. DR3) had scatter at lower doses that suggests the potential for post-depositional mixing (e.g., bioturbation or cryoturbation) thus OSL dating of this sample was considered unreliable. The central age model (CAM; Galbraith et al., 1999) was used to determine an age for sample KQ2 as the symmetrical D_e distribution suggests that these grains were not heterogeneously bleached prior to burial. The minimum age model (MAM; Galbraith et al., 1999; Galbraith and Laslett, 1993) was used to determine

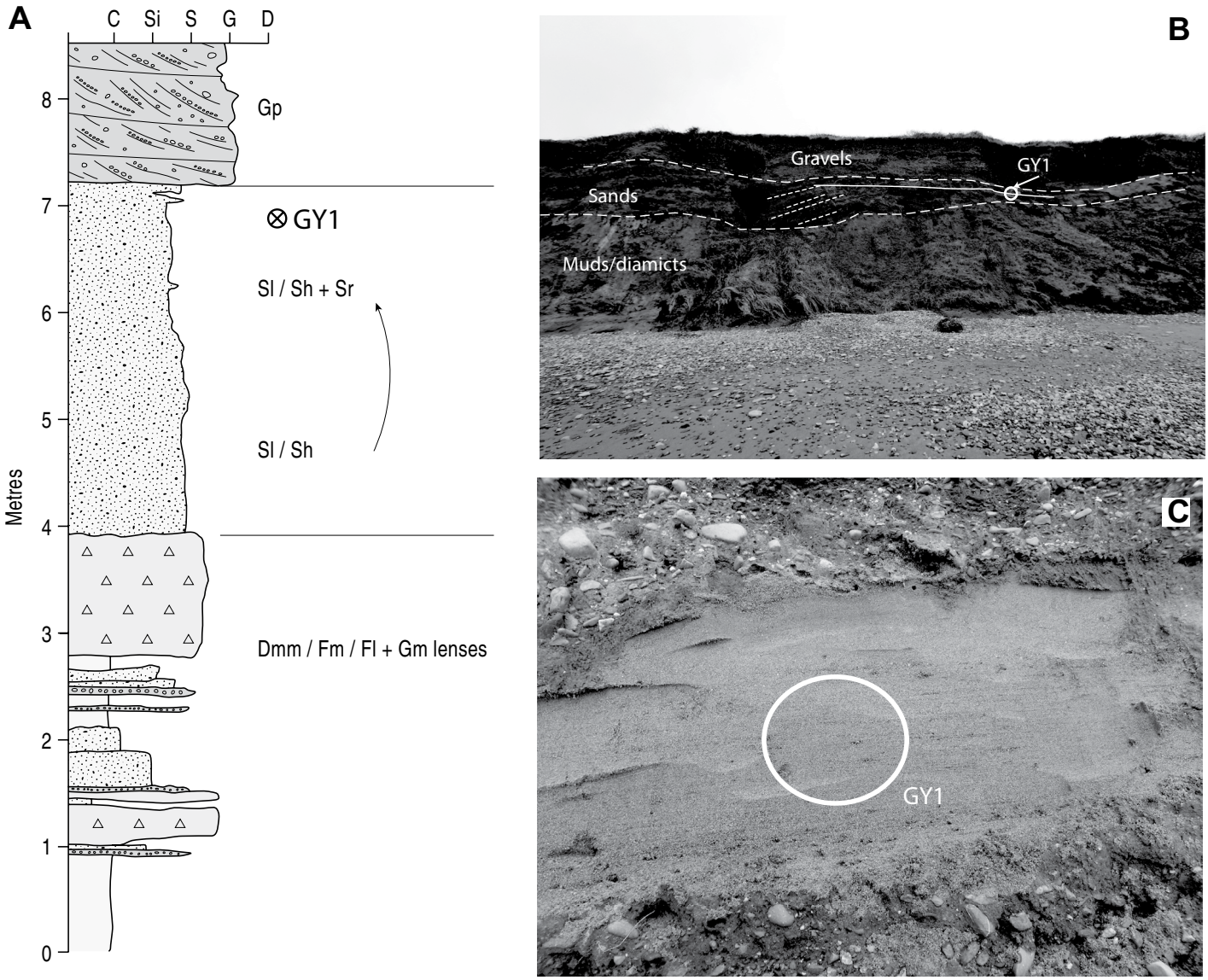

Figure 8. (A) Stratigraphic log of Greystones, Co. Wicklow, Ireland, section from McCabe and Ó Cofaigh (1995) with optically stimulated luminescence (OSL) sample location indicated. (B) Photograph of sampled section. Gravel foresets of Gilbert-like delta shown with angled dashed white lines (this was not described by McCabe and Ó Cofaigh [1995]). Thin continuous white line shows continuous sand bed sampled for OSL dating. (C) Sample GR1 within a thin sand bed ~40 cm thick. Note gravels above and below.

ages for the remaining samples given their asymmetrical D_e distributions (Duller, 2008). The D_e values were then divided by the dose-rate to determine an age. See the GSA Data Repository for full details of the OSL analysis performed in this study, in addition to the D_e values determined for each sample.

Cosmogenic Nuclide Exposure Dating

Sampling targeted the uppermost fresh surfaces of boulders and bedrock to minimize the possibility of post-depositional adjustment such as toppling or large scale spallation of bedrock. Topographic shielding was measured in the field using a compass and clinometer and correction factors calculated using the CRONUS-Earth online calculator (Balco et al., 2008). CN sample preparation was undertaken at the University of Glasgow, Scotland, UK, using standard mineral separation techniques (cf. Kohl and Nishiizumi, 1992). Beryllium extraction was carried out at the Cosmogenic Isotope Analysis Facility–Scottish Universities Environmental Research Centre (CIAF-SUERC), using procedures based on Child et al. (2000). The $^{10}Be/^{9}Be$ ratios were measured on the 5MW accelerator mass spectrometer (AMS) at SUERC (Xu et al., 2010).

There are a variety of online calculators (Balco et al., 2008; Marrero et al., 2016; Martin et al., 2017), scaling schemes (e.g., Lal, 1991; Lifton et al., 2014; Stone, 2000), and production rate calibrations (e.g., Putnam et al., 2010; Small and Fabel, 2015; Young et al., 2013) available for calculating exposure ages. We present exposure ages calculated using the CRONUS-Earth calculator (Balco et al., 2008) and the CRONUScalc calculator (Marrero et al., 2016) using a selection of scaling schemes (Lm [Lal, 1991; Stone, 2000] and SA [Lifton et al., 2014]) and production rates (Borchers et al., 2016; Fabel et al., 2012). In practice, choice of calculation method and scaling scheme often make little difference for calculation of ^{10}Be exposure ages (cf. Table 4). Choice of production

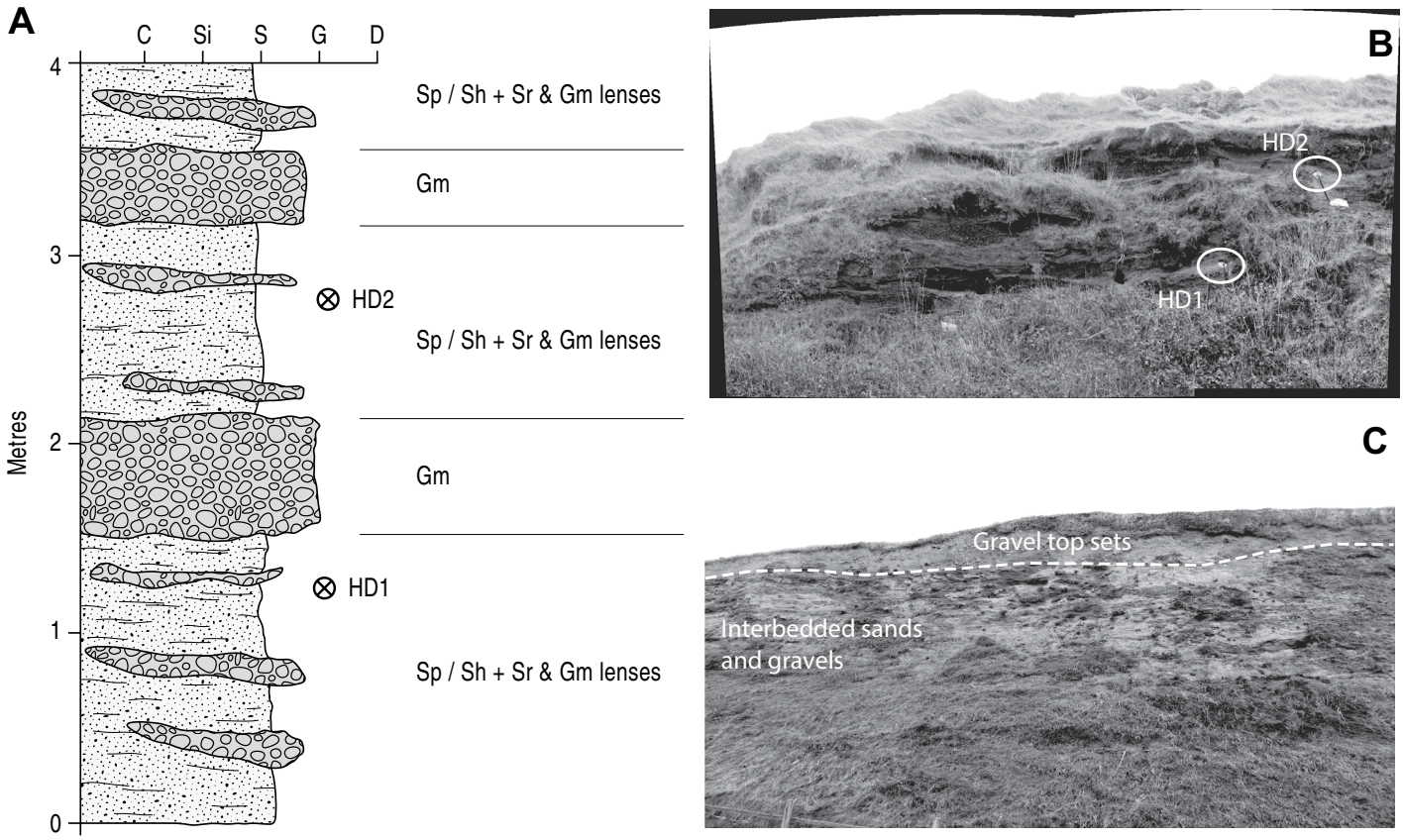

Figure 9. (A) Stratigraphic log of sampled section on Howth Delta, Co. Dublin, Ireland, with location of optically stimulated luminescence (OSL) samples indicated. (B) Photograph of sampled section with locations of samples shown. (C) Flow parallel section exposed in nearby road cutting showing alternating sand and gravel beds with gravel top sets. Section is ~15 m high.

rate, however, can make a significant difference and affect subsequent interpretations. Given an apparent geographical bias on production rate values (Phillips et al., 2016) it has been argued that ages should be calculated using the most geographically appropriate calibration (Small and Fabel, 2016a). Considering this, and to aid comparison to previously published work from Britain and Ireland, we focus discussion on ages calculated with the CRONUS calculator (http://hess.ess.washington.edu; Balco et al., 2008), the Lm scaling, and with a reference sea-level high latitude production rate of 4.00 ± 0.17 atoms g^{-1} quartz (cf. Fabel et al., 2012) calibrated from a site in Scotland, <500 km from our study site.

Bayesian Age Modeling

Integration of the new CN and OSL age control was undertaken using Bayesian age modeling, with the focus on discerning the timing of ice marginal retreat. A sequence model was used which requires the dating information to be arranged in a likely younging order irrespective of the actual age values; this *prior* model (the hypothetical relative order of events) takes the form of a south to north relative distance reconstruction of retreat of the ISIS margin (Fig. 2). The Bayesian modeling was conducted using OxCal 4.3 (Bronk Ramsey, 2017) and run in an outlier mode (Buck et al., 1991; Bronk Ramsey, 2009) to assess for outliers in *time (t)* with outlier probabilities assigned a minimum outlier probability of 0.05 which was increased on the basis of quality assurance criteria (see Small et al., 2017). This approach allows all data to be included within the model (suitably down-weighted) and removes the need for the somewhat subjective approach of identifying and removing outliers. The likelihood data—or age measurements—were expressed as a Student's *t*-distribution (more long-tailed than a normal distribution) and attributed an outlier scaling of 10^0–10^4 years (cf. Bronk Ramsey, 2009). The model (see GSA Data Repository for code) was punctuated by uniform in shape prior boundaries that separate a series of phases, essentially an unordered group of likelihoods—or age measurements—for individual locations. The modeled boundary ages document the retreat of the ISIS and allow rates of retreat between boundaries to be calculated.

However, the Bayesian approach to constraining ice margin retreat assumes uni-directional ice retreat (i.e., from south to north in this case). Consequently, any unidentified large scale readvances would cause the reconstructed retreat rates to underestimate the maximum retreat rate experienced by the ice margin between any two given Bayesian boundaries. Similarly, any stillstands or periods of ice margin oscillation will have a similar effect. It therefore must be highlighted that the reconstructed retreat rates presented here represent time-averaged retreat rates between the Bayesian boundaries and that the actual rate likely varied by an unquantifiable amount to be both faster and slower than the time averaged rate. However, given the scale of the transect (~175 km), and the duration of retreat (ca. 7 ka) we consider that time averaged rates provide useful context for modern day retreat rates and for comparison to paleo-ice sheet model output. Additionally, given the lack of evidence for large scale readvances in this sector of the ISB we infer that the time averaged retreat rates presented are a reasonable approximation of the true retreat rate of the ISIS.

TABLE 3. CHEMISTRY AND DOSE RATE DATA OF OPTICALLY STIMULATED LUMINESCENCE SAMPLES

Short sample code	Depth (m)	Water content (%)*	K (%)	Rb (ppm)	U (ppm)	Th (ppm)	External beta dose-rate (Gy/ka) †	External gamma dose-rate (Gy/ka)	External cosmic dose-rate (Gy/ka)§	Total dose-rate (Gy/ka) #	Age model	σ_b	D_e (Gy)	Age (ka)
KQ1	1.5	23 ± 5	1.1 ± 0.1	44.9 ± 4.5	1.1 ± 0.1	4.9 ± 0.5	0.83 ± 0.08	0.58 ± 0.04	0.17 ± 0.02	1.60 ± 0.09	MAM	0.45	41.2 ± 7.2	25.7 ± 4.7
KQ2	2.0	23 ± 5	1.0 ± 0.1	37.9 ± 3.8	1.3 ± 0.1	3.9 ± 0.4	0.75 ± 0.07	0.44 ± 0.03	0.16 ± 0.02	1.37 ± 0.08	CAM	N.A	35.8 ± 2.3	26.2 ± 2.2
BW1	12.0	20 ± 5	0.5 ± 0.1	19.6 ± 2.0	0.6 ± 0.1	1.8 ± 0.2	0.38 ± 0.04	0.23 ± 0.02	0.05 ± 0.01	0.67 ± 0.04	MAM	0.20	26.1 ± 3.2	37.1 ± 5.0
BW2	10.0	20 ± 5	0.4 ± 0.1	16.7 ± 1.7	0.5 ± 0.1	1.6 ± 0.2	0.30 ± 0.03	0.20 ± 0.01	0.06 ± 0.01	0.58 ± 0.03	MAM	0.20	15.2 ± 1.8	24.9 ± 3.3
KS1	11.0	20 ± 5	0.8 ± 0.1	28.2 ± 2.8	0.6 ± 0.1	1.9 ± 0.2	0.56 ± 0.06	0.32 ± 0.02	0.03 ± 0.00	0.91 ± 0.06	MAM	0.25	21.4 ± 3.2	22.7 ± 3.7
KS2	10.0	20 ± 5	0.4 ± 0.1	16.7 ± 1.7	0.4 ± 0.1	1.5 ± 0.2	0.30 ± 0.03	0.23 ± 0.02	0.06 ± 0.01	0.60 ± 0.03	MAM	0.25	18.5 ± 2.5	28.7 ± 4.2
BV1	9.0	20 ± 5	0.4 ± 0.1	13.9 ± 1.4	0.4 ± 0.1	1.6 ± 0.2	0.30 ± 0.03	0.20 ± 0.01	0.07 ± 0.01	0.58 ± 0.03	MAM	0.35	13.4 ± 2.8	21.8 ± 4.7
TB1	9.0	20 ± 5	1.1 ± 0.1	41.7 ± 4.2	1.2 ± 0.1	3.9 ± 0.4	0.82 ± 0.08	0.44 ± 0.03	0.07 ± 0.01	1.34 ± 0.08	MAM	0.35	32.3 ± 4.5	24.0 ± 3.7
TB2	19.0	23 ± 5	0.7 ± 0.1	28.1 ± 2.8	0.7 ± 0.1	2.4 ± 0.2	0.50 ± 0.05	0.32 ± 0.02	0.03 ± 0.00	0.89 ± 0.05	MAM	N.A	N.A	N.A
BH1	17.5	20 ± 5	1.1 ± 0.1	47.4 ± 4.7	1.5 ± 0.2	4.3 ± 0.4	0.85 ± 0.08	0.54 ± 0.04	0.03 ± 0.00	1.44 ± 0.09	MAM	0.30	26.0 ± 3.8	18.1 ± 2.9
BH2	17.5	20 ± 5	1.1 ± 0.1	46.0 ± 4.6	1.3 ± 0.1	3.5 ± 0.4	0.82 ± 0.08	0.47 ± 0.03	0.03 ± 0.00	1.34 ± 0.08	MAM	0.30	32.1 ± 4.9	24.0 ± 4.0
GY1	5.0	30 ± 5	1.2 ± 0.1	55.6 ± 5.6	1.4 ± 0.1	3.0 ± 0.3	0.80 ± 0.08	0.43 ± 0.03	0.11 ± 0.01	1.35 ± 0.08	MAM	0.20	22.9 ± 2.7	16.9 ± 2.3
HD1	5.0	20 ± 5	1.1 ± 0.1	41.3 ± 4.1	1.3 ± 0.1	4.1 ± 0.4	0.83 ± 0.08	0.51 ± 0.03	0.11 ± 0.01	1.47 ± 0.09	MAM	0.30	31.4 ± 4.9	21.4 ± 3.6
HD2	1.5	20 ± 5	1.1 ± 0.1	42.7 ± 4.3	1.4 ± 0.1	4.4 ± 0.4	0.84 ± 0.08	0.52 ± 0.03	0.17 ± 0.02	1.55 ± 0.09	MAM	0.30	39.7 ± 4.7	25.6 ± 3.3

*Water contents are expressed as a percentage of the mass of dry sediment.
†External dose-rates calculated using the conversion factors of Guérin et al. (2011) and beta dose-rate attenuation factors of Guérin et al. (2012).
§Cosmic dose-rates were calculated after Prescott and Hutton (1994).
#Dose-rates were calculated using the Dose Rate and Age Calculator (DRAC; Durcan et al., 2015).

DATING RESULTS

Luminescence Ages

The new OSL ages range from 37.1 to 16.9 ka (Fig. 10; Table 3). There was agreement within uncertainties for the two OSL ages determined for sediments from each site—Kilmore Quay, Knocknasillogue, Ballyhorsey, Howth Delta—except for Blackwater. At Blackwater, the OSL age for sample BW1 (37.1 ± 5.0 ka) was older than sample BW2 (24.9 ± 3.3 ka). Both samples were heterogeneously bleached prior to burial, thus the difference in OSL ages is potentially due to the minimum dose population in the single-grain D_e distribution of sample BW1 not being as well characterized as sample BW2. It is therefore likely that deglaciation at Blackwater is more accurately constrained by the OSL age for sample BW2 (24.9 ± 3.3 ka). This is supported by the fact that the mean age of BW1 (37.1 ka) pre-dates the timing of the ISIS maximum extent. Additionally, the OSL ages for sites to the south (Kilmore Quay) and north (Knocknasillogue) of Blackwater, which constrain the timing of ice-marginal retreat across this transect are consistent with the younger (BW2) age. The OSL ages determined for individual samples from Ballyvaldon (21.8 ± 4.7 ka), Tinnaberna (24.0 ± 3.7 ka), and Greystones (16.9 ± 2.3 ka) are also—within uncertainties—in agreement with the conceptual model of deglaciation relative to the OSL ages at Kilmore Quay, Knocknasillogue, Ballyhorsey, and Howth.

Cosmogenic Exposure Ages

The cosmogenic ages obtained span the range of 27.8–11.4 ka (Table 4; Fig. 10) and show significant variation within individual sites. Only at Bray Head do two samples (BR1 and BR3) agree within their 1σ analytical uncertainties, where the mean age (20.7 ± 1.1 ka) represents the best estimate of the deglaciation age. We note that BR2 was collected from an abraded bedrock surface that is more likely to be influenced by inheritance (Briner and Swanson, 1998) compared to the boulder and plucked bedrock samples (Colgan et al., 2002; Putkonen and Swanson, 2003; Heyman et al., 2011). Of the exposure ages from the other sites some are likely erroneous. CS1 has an apparent exposure age that post-dates the termination of the Younger Dryas at which point Britain and Ireland were ice free (Bromley et al., 2014; Small and Fabel, 2016b). CS2 has an apparent exposure age that pre-dates both initial advance of the ISIS (Ó Cofaigh and Evans, 2007) and the timing of maximum extent on the Isles of Scilly (Smedley et al., 2017a). These ages are down-weighted accordingly in the subsequent Bayesian model (cf. Small et al., 2017).

TABLE 4. ^{10}BE CONCENTRATIONS AND EXPOSURE AGES REPORTED IN THIS STUDY

			CRONUS-Earth (Lm)*		CRONUScalc (Lm)†		CRONUScalc (SA)†	
Sample	Be conc.	±	Age (ka)	±	Age (ka)	±	Age (ka)	±
Carnsore Point								
CS1	45067	1940	11.4	0.7 (0.5)	11.0	1.0 (0.5)	11.0	1.0 (0.5)
CS2	107506	3110	27.8	1.5 (0.8)	27.3	2.3 (0.8)	27.0	2.2 (0.8)
CS3	95112	3022	24.0	1.3 (0.8)	24.0	2.0 (0.8)	23.4	1.9 (0.7)
Wicklow Meltwater Channel								
WK1	64608	2403	19.7	1.2 (0.7)	19.5	1.7 (0.7)	19.3	1.6 (0.7)
WK2	72855	2027	22.3	1.2 (0.6)	22.1	1.8 (0.6)	21.8	1.8 (0.6)
Bray Head								
BR1	98816	3406	20.1	1.1 (0.7)	19.8	1.7 (0.7)	19.9	1.6 (0.7)
BR2	113650	3916	23.3	1.3 (0.8)	23.0	2.0 (0.8)	22.9	1.9 (0.8)
BR3	104999	3003	21.5	1.1 (0.6)	21.1	1.8 (0.6)	21.2	1.7 (0.6)
Hill of Howth								
HO1	118816	3374	25.6	1.4 (0.7)	25.1	2.1 (0.7)	25.0	2.0 (0.7)
HO2	98103	3600	21.2	1.2 (0.8)	20.8	1.8 (0.8)	20.8	1.7 (0.8)

Note: Numbers in parentheses are 1σ analytical uncertainties.

*Calculated using CRONUS calculator; Wrapper script 2.3, Main calculator 2.1, Constants 2.3, Muons 1.1 (Balco et al., 2008). See text for details of production rates. Ages assume 1 mm ka^{-1} erosion, no inheritance, and density of 2.65 g cm^{-3}.

†Calculated using CRONUScalc v.2 calculator (Marrero et al., 2016). Details of production rates in Borchers et al. (2016). Ages assume 1 mm ka^{-1} erosion, no inheritance, and density of 2.65 g cm^{-3}.

Bayesian Age Modeling

The geochronological data above do not exist in isolation but are accompanied by spatial information (the "prior model") that places dated sites within a morpho-stratigraphical order representing a series of ice-marginal positions arranged in the order of ice margin retreat (cf. Chiverrell et al., 2013). This independently constructed relative order of events (Fig. 2) constrains the independent age measurements with overlapping age probability distributions providing the basis for using Bayesian age modeling (Buck et al., 1991; Bronk Ramsey, 2009). Bayesian age modeling produced a conformable sequence with an agreement index exceeding the threshold of 60 as defined by Bronk Ramsey (2009) (Fig. 11; Table 5). Assigning increased outlier probabilities for those samples where *posterior likelihood* > *prior likelihood* did not result in any significant differences in age model output.

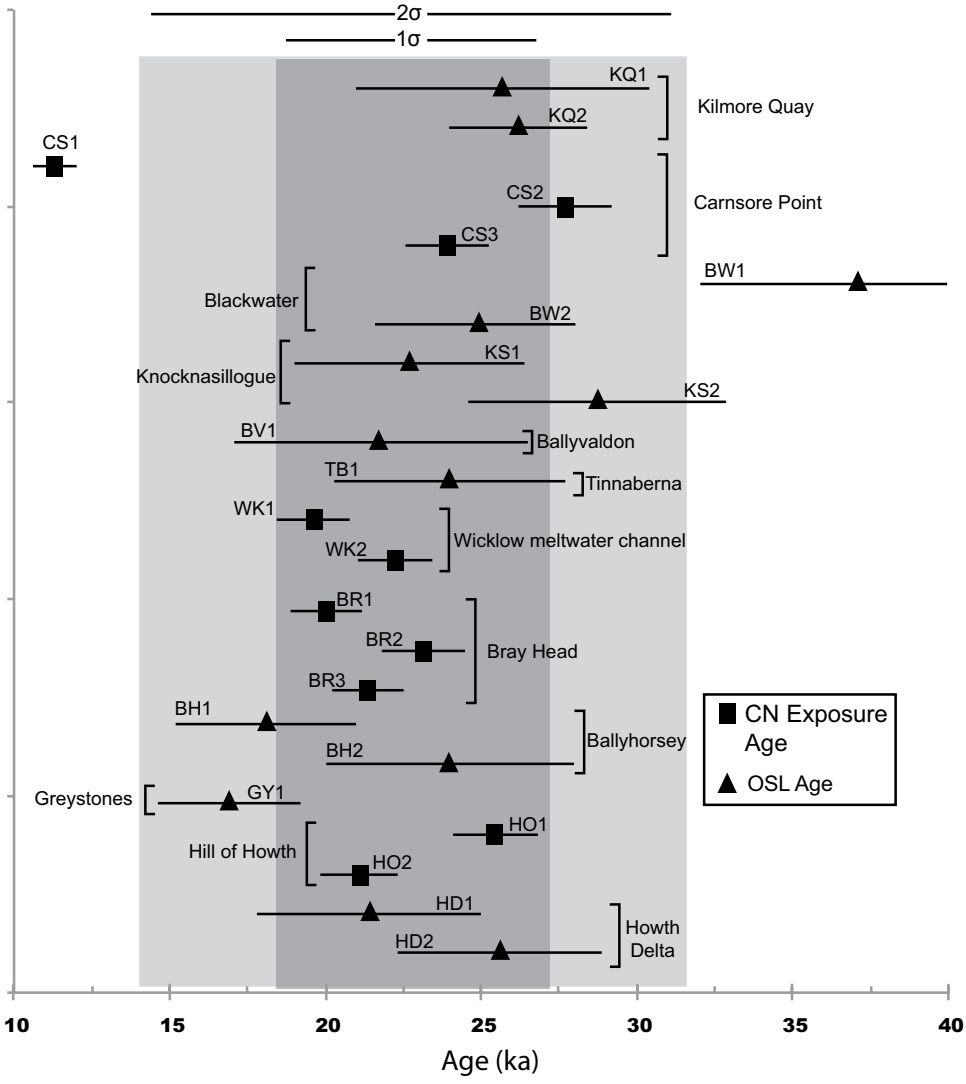

Figure 10. Summary plot of all optically stimulated luminescence (OSL) and cosmogenic nuclide (CN) ages discussed in the text. Dark and light boxes denote ± 1σ and ± 2σ of the whole population. Note that only two ages (CS1 and BW1) lie outside the ± 2σ range.

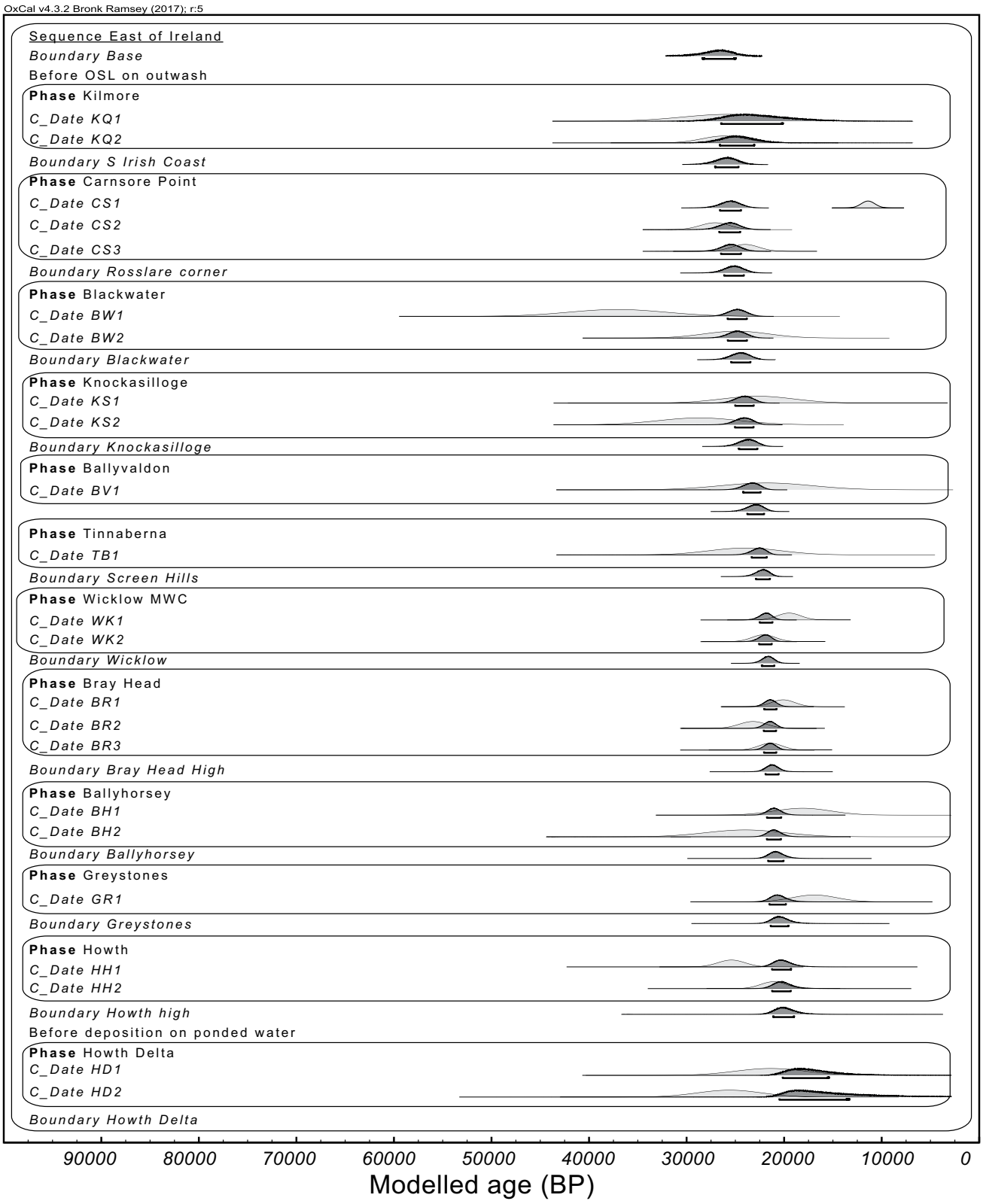

Figure 11. Bayesian sequence model of the new dating control for the paleo–Irish Sea Ice Stream and the OxCal keywords that define the relative order (*prior*) model (Bronk Ramsey, 2009). Each distribution (light gray) represents the relative probability of each age estimate with posterior density estimate (dark gray) generated by the modeling. Outlier coding denotes dating information excluded or down-weighted in the modeling. OSL—optically stimulated luminescence; MWC—Wicklow meltwater channel.

The model produces a conformable sequence with modeled boundary ages for all sample sites. These ages range from 26.6 ± 1.9 ka to 19.5 ± 1.3 ka (Table 5). Additionally, the model produces boundary ages that have significantly lower uncertainties than the best estimate deglaciation ages produced by geochronological dating for sites where there was agreement between ages.

Our Bayesian age model indicates that initial ice marginal retreat onto the southern Irish coast occurred at 25.9 ± 1.4 ka (Boundary 2). Retreat of the ISIS from the southern coast of Ireland is constrained by the modeled age (Boundary 3) of 25.1 ± 1.2 ka. Deglaciation to the Wexford coast, and associated deposition of the Screen Hills complex, occurred between 24.2 ± 1.2 ka and 22.1 ± 0.7 ka (Boundaries 4–7). Subsequent deglaciation of the eastern coast of Ireland is constrained by modeled ages from Wicklow Point, Bray Head, Greystones, and the Howth Peninsula and occurred between 21.6 ± 0.6–20.1 ± 1.0 ka (Boundaries 8–12). Final deglaciation of the portion of the ISIS contained within our prior model was complete by 19.5 ± 1.3 ka, when deposition of the Howth Delta occurred (Boundary 13). These modeled age boundaries can be interpreted in terms of the timing of retreat of the lateral margin of the ISIS along the south and east coasts of Ireland and used to test our conceptual model of ISIS deglaciation.

TABLE 5. BOUNDARY NAMES, GEOCHRONOLOGICAL AGES, AND BAYESIAN BOUNDARY AGES (1Σ)

Boundary	Site	Cumulative retreat distance (km)	Samples	Ages (ka)	±	Boundary ages (ka)	±
Boundary Base (1)	N.A	N.A	N.A	N.A	N.A	26.6	1.9
Boundary S Irish Coast (2)	Kilmore Quay	0	KQ1	25.7	4.7	25.9	1.4
			KQ2	26.2	2.2		
Boundary Rosslare corner (3)	Carsnsore Point	22	CS1	11.4	0.7	25.1	1.2
			CS2	27.8	1.5		
			CS3	24.0	1.3		
Boundary Blackwater (4)	Blackwater	45	BW1	37.1	5.0	24.2	1.2
			BW2	24.9	3.3		
Boundary Knocknasillogue (5)	Knocknasillogue	47	KS1	22.7	3.7	23.6	1.1
			KS2	28.7	4.2		
Boundary Ballyvaldon (6)	Ballyvaldon	50	BV1	21.8	4.7	22.8	0.9
Boundary Screen Hills (7)	Tinnaberna	52	TB1	24.0	3.7	22.1	0.7
Boundary Wicklow (8)	Wicklow MWC	128	WK1	19.7	1.2	21.6	0.6
			WK2	22.3	1.2		
Boundary Bray Head high (9)	Bray Head	153	BR1	20.1	1.1	*21.2*	*0.7*
			BR2	23.3	1.3		
			BR3	21.5	1.2		
Boundary Ballyhorsey (10)	Ballyhorsey	142	BH1	18.1	2.9	20.8	0.8
			BH2	24.0	4.0		
Boundary Greystones (11)	Greystones	151	GY1	16.9	2.3	20.5	0.8
Boundary Howth high (12)	Hill of Howth	171	HO1	25.4	1.4	*20.1*	*1.0*
			HO2	21.1	1.2		
Boundary Howth (13)	Howth Delta	173	HD1	21.4	3.6	19.5	1.3
			HD2	25.6	3.3		

Note: Numbers in parentheses correspond to Boundary numbers in Figures 1 and 2. Boundaries in italics denote modelled ages not used to calculate time averaged retreat rates. MWC–meltwater channel.

DISCUSSION

Retreat Rate along the Lateral Margin of the Irish Sea Ice Stream

Retreat rates for the ISIS (Table 6) were derived from the mean modeled boundary ages and evidence major changes in the pace of marginal retreat displayed by the ISIS. We separate ISIS marginal retreat into four distinct stages. *Stage I* (25.9–24.2 ka) deglaciation proceeds at a near constant rate of ~26 m a^{-1} with the margin passing from Kilmore Quay (*S Irish Coast*) to Carnsore Point (*Rosslare corner*) and then to Blackwater Harbour (*Blackwater*). During *Stage 2* (24.2–22.1 ka; *Blackwater–Screen Hills*) modeled rates of ISIS axial margin retreat exhibit an order of magnitude slowing at the Screen Hills (Table 6) from ~26 m a^{-1} to ~3 m a^{-1}. In this deceleration the ISIS ice margin would have likely experienced numerous stillstands and readvances, which is in accordance with sedimentological and geomorphological evidence for repeated ice margin re-advance in the Screen Hills area (Thomas and Summers, 1983, 1984). Similarly, the relatively rapid rates of retreat onto and along the south coast of Ireland accord well with the sedimentological evidence suggesting the first major slowing of ice marginal retreat was in close proximity to the Screen Hills (cf. Thomas and Summers, 1983, 1984; Thomas and Kerr, 1987; Ó Cofaigh and Evans, 2001a, 2001b; Evans and Ó Cofaigh, 2003; Thomas and Chiverrell, 2011). During *Stage 3* (22.1–21.6 ka; *Screen Hills–Wicklow*) retreat of the axial ice margins proceeded rapidly at average rates of 152 m a^{-1} (Table 6) and there are no reported substantial ice marginal landforms or accumulations of glacial deposits; this is commensurate with rapid ISIS retreat. This retreat phase (*Stage 3*) accounts for 75 km of the total 173 km of ISIS axial retreat in the ISB. Ice marginal retreat during *Stage 4* (21.6–19.5 ka; *Wicklow–Howth*) is less rapid at ~21 m a^{-1}, supporting sedimentological evidence for ice margin stillstands at Greystones (McCabe and Ó Cofaigh, 1995), and oscillatory ice marginal retreat at Killiney (Rijsdijk et al., 2010). In summary, there is a strong correspondence between the modeled rates of ISIS marginal retreat and our conceptual model inferred from the geomorphology and stratigraphy (Fig. 2).

Ice stream Behavior: External Forcing or Internal Dynamics?

Our modeled boundary age for ISIS deglaciation of the south Irish coast (24.5 ± 1.5 ka) is indistinguishable from the existing geochronology constraining the advance to, and maximum extent of, the ISIS (Ó Cofaigh and Evans, 2007; Ó Cofaigh et al., 2012; Smedley et al., 2017a). Our data and the existing chronology suggest that the advance to, and retreat from, maximum extent (total distance of ~600 km) occurred within 1–2 ka (i.e., within the resolution of the

TABLE 6. TIME AVERAGED RETREAT RATES BETWEEN *(I)* INDIVIDUAL BAYESIAN BOUNDARIES AND *(II)* THE RETREAT STAGES IDENTIFIED BASED ON THE MEDIAN AGE OF MODELLED AGE DISTRIBUTION

(i) Boundary retreat (boundary numbers)	Cumulative retreat (km)	Individual retreat rates (m a^{-1})	*(ii)* Retreat stages	Average retreat rate (m a^{-1})
S Irish coast (2)–Rosslare corner (3)	22	28	*Stage I*	26
Rosslare corner (3)–Blackwater (4)	45	26	*(S Irish Coast–Blackwater)*	
Blackwater (4)–Knocknasillogue (5)	47	3	*Stage II*	3
Knocknasillogue (5)–Ballyvaldon (6)	50	4	*(Blackwater–Screen)*	
Ballyvaldon (6)–Screen Hills (7)	52	3		
Screen Hills (7)–Wicklow (8)	128	152	*Stage III (Screen–Wicklow)*	152
Wicklow (8)–Ballyhorsey (10)	142	18	*Stage IV*	21
Ballyhorsey (10)–Greystones (11)	151	30	*(Wicklow–Howth)*	
Greystones(11)–Howth (13)	173	22		

available geochronology) and, assuming equal time for both components, this points to axial retreat rates of 300–600 m a^{-1}. These are an order of magnitude higher than those observed during our *Stage 1* (*S Irish Coast–Blackwater*; 25.9–24.2 ka) and we suggest that this reduction of the retreat rates reflects the continued narrowing of the calving margin width toward and into St George's Channel. Given the short duration but extensive nature of ISIS maximum advance, it likely reflects a dynamic instability within the ice sheet during growth leading to rapid advance and probably over-extension such that the ice stream extended far beyond any position that can be reconciled with a glacial system in which accumulation and ablation were in equilibrium. Rapid or surge-like advances of the ISIS into the Celtic Sea have previously been inferred from marine cores (Scourse et al., 1990). The ISIS at maximum extent, given its axial length, would have had a low profile and been thin at its margin (cf. Scourse et al., 1990), and in advancing from the topographic constriction of St George's Channel it spread out as a piedmont-like lobe. This low gradient, thin-ice and wide calving margin configuration likely rendered an over-extended ISIS vulnerable to rapid retreat perhaps conditioned by accelerated calving but driven by factors such as glaci-eustatic changes, a warmer sea surface, a megatidal regime and/or increasing air temperature leading to hydrofracturing (Haapaniemi et al., 2010; Scourse et al., 2009, 2018; Pollard et al., 2015). Notwithstanding limits imposed by uncertainties of the modeled chronology, the ISIS advance and retreat back to the south coast of Ireland by ca. 24.5 ka appears to pre-date any significant climate/oceanic warming in the North Atlantic (i.e., Greenland Interstadial 2; GI-2; 23.3–22.9 ka b2k; Rasmussen et al., 2014). However, even without external climate forcing at maximum extent, the ISIS may have been intrinsically unstable as thin ice masses near buoyancy are vulnerable to full-thickness tensile failure which would also lead to accelerated calving (Ma et al., 2017).

Slowing of ice margin retreat (*Stage 2; Blackwater–Screen Hills*) in our modeled chronology between 24.2 ± 1.2 ka and 22.1 ± 0.7 ka corresponds with transit of the ISIS margin into the narrowing of the St George's Channel and the onset of minor readvance episodes and still-stands on the lateral ISIS margin at the Screen Hills. The Screen Hills mark a step-change in the ISIS axial trough geometry, with narrowing of the potential calving margin and a shallower trough depth (Fig. 12). These likely changes would have reduced the lateral and vertical extent of the calving margin, thus reducing calving rates leading to stabilization of the ice margin. A similar scenario of ice margin stabilization at trough constrictions was present in numerical modeling of the Marguerite Bay Ice Stream (Jamieson et al., 2012) and has been widely recognized in the literature (e.g., Benn et al., 2007). When an ice stream stabilizes at a trough constriction it ceases to thin at the grounding line although longitudinal stress coupling acts to propagate thinning up stream (Payne et al., 2004; Jamieson et al., 2012). This mechanism can fundamentally limit the duration of stability as the upstream drawdown can only deliver ice to the grounding line for as long as the source areas maintain sufficient ice storage. Such a scenario of drawdown would likely be accompanied by faster flow linked to accelerated ice flux

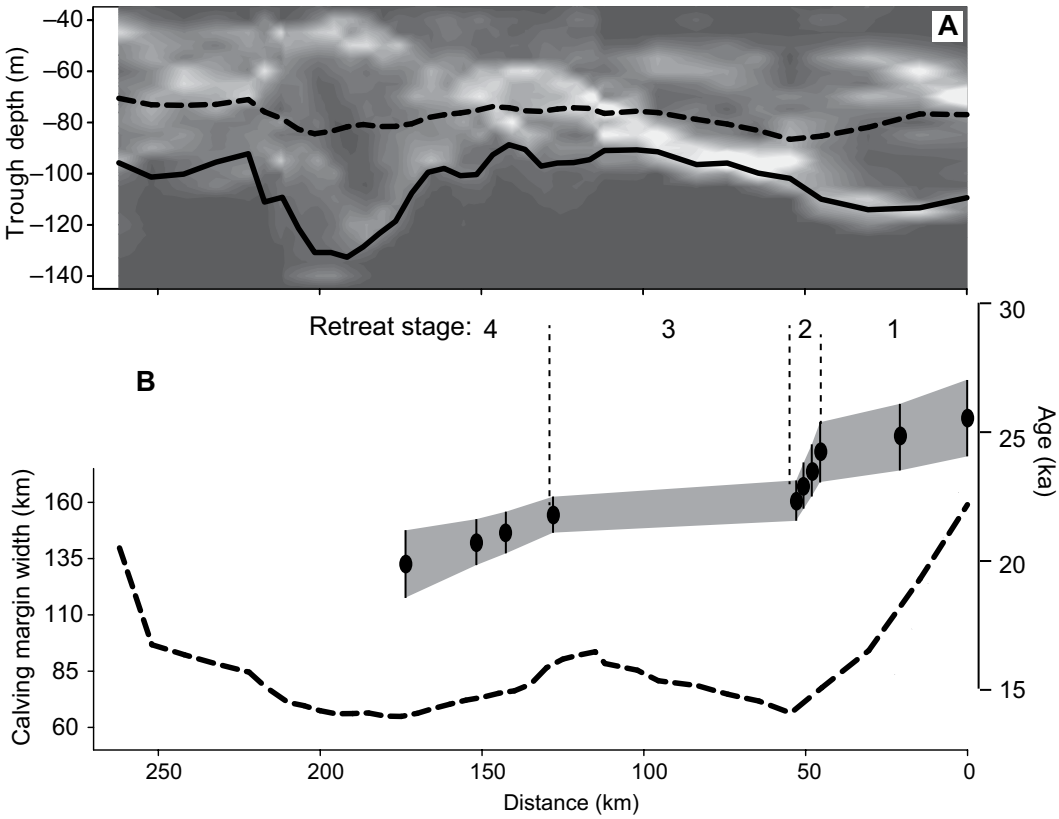

Figure 12. Modeled boundary age distributions plotted against (A) trough depth. The contour plot displays the depth distribution measured parallel to trough axis distance as shown in Figure 1. Thus, lighter colors indicate increased frequency of any given depth. The solid black line is the 90th percentile of the overall depth distribution at any given axial retreat distance, a proxy for maximum trough depth. The dashed black line is the mean trough depth at any given distance. As an example of how to interpret this plot at 0 km the maximum trough depth is relatively deep (~115 m) compared to the mean depth and the highest frequency occurrence of the overall depth distribution. (B) Calving margin width defined as the distance between the –50 m isobath along the axis of retreat. Note the change in trough geometry in the area of the Screen Hills (Retreat stage 2), near the south east coast of Ireland, where the calving margin width reaches a minimum in the constriction of the St George's Channel and there is a step change in the depth distribution.

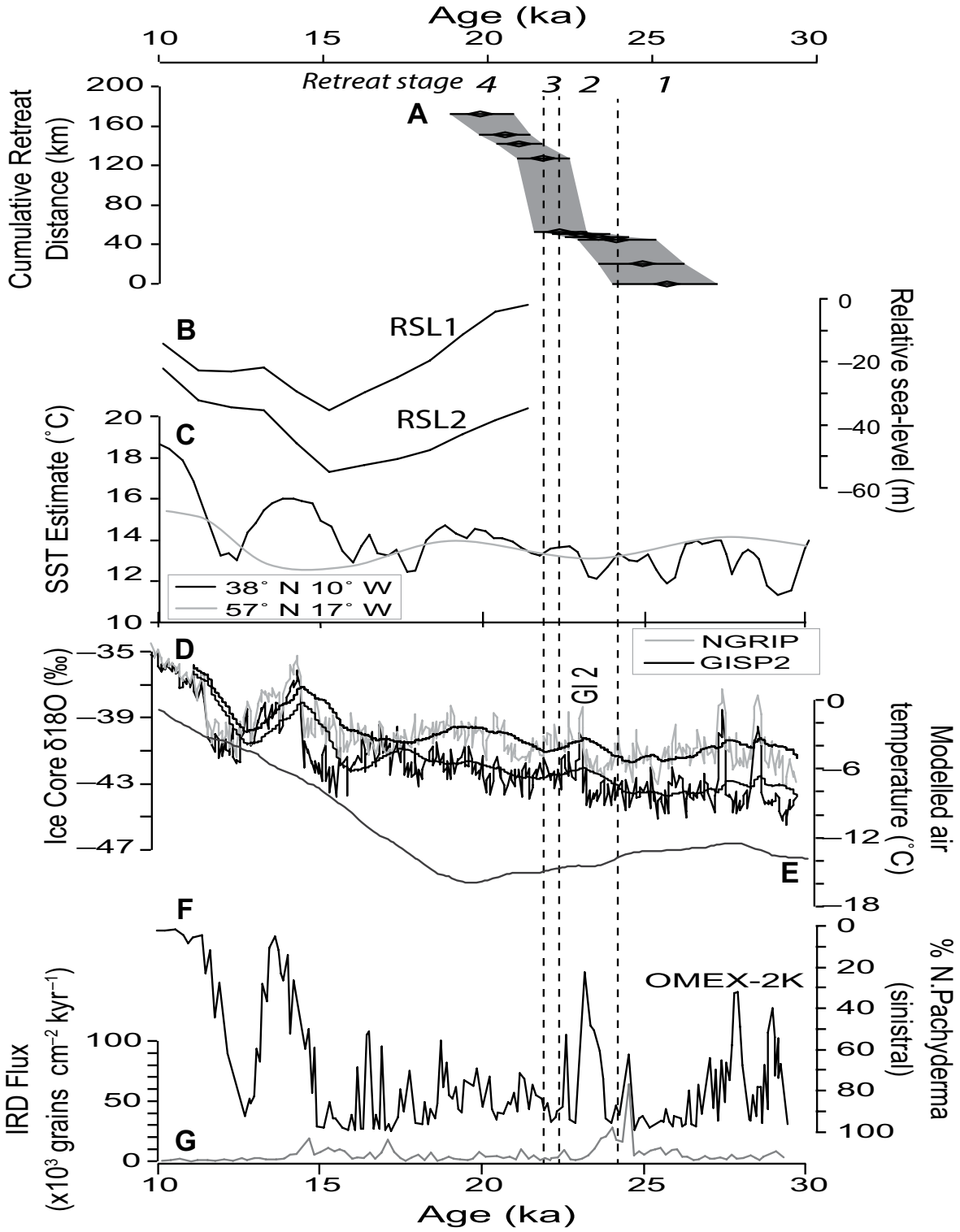

Figure 13. Proxy records of potential deglacial forcing for the time period of the Irish Sea Ice Stream deglaciation. (A) Retreat stages as inferred from modeled boundary ages are indicated by the dashed lines. (B) Glacial isostatic adjustment (GIA) generated predictions of relative sea level change based on Bradley et al. (2011). The locations of RSL1 and RSL2 are shown on Figure 1. (C) Sea surface temperature (SST) estimates at 37°N 10°W (Bard, 2002; Bard et al., 2004) and 57°N 17°W (Lawrence et al., 2009). (D) Greenland oxygen isotope records ($\delta^{18}O$, ‰) from NGRIP and GISP2 on the GICC05 timescale (Rasmussen et al., 2014; Seierstad et al., 2014) (50 year moving averages shown by black lines). (E) Modeled surface-air temperatures relative to present for land masses north of ~45°N (Bintanja et al., 2005). (F) *% N. pachyderma* (sinistral) and (G) total Ice Rafted Detritus (IRD) flux (>150 μm cm^{-2} ka^{-1}) from OMEX-2K core at 49°N 13°W (Haapaniemi et al., 2010).

to the grounding line. Geophysical evidence for ice streaming occurs immediately to the north of our region in the central ISB (Van Landeghem et al., 2009) providing evidence for fast-flow, potentially while the ice margin was located at the Screen Hills. Continued ice sheet drawdown would cause the ISIS to become increasingly sensitive to external perturbations that act to increase mass loss at the grounding line as eventually there would be insufficient upstream mass to sustain fast flow. However, the switch from slower oscillating ice margin behavior (*Stage 2*) to more rapid marginal retreat (*Stage 3*) at 22.1 ka appears to post-date GI-2 (23.3–22.9 ka; Fig. 13A), a time of ocean warming in the North Atlantic cited as a potential major driver of BIIS deglaciation (Scourse et al., 2009). Additionally, given that modeled relative sea levels are falling at 21 ka (Bradley et al., 2011; Fig. 13B) it is reasonable to assume that a rise in relative sea-level capable of triggering rapid ice margin retreat was unlikely to have occurred prior to 21 ka. Thus, both the slow-down of marginal retreat and later acceleration of retreat rates display an apparent poor coupling to ocean-climate forcing in the North Atlantic.

More rapid retreat (*Stage 3*) continues across a normal bed-slope that shallows in the direction of retreat (Fig. 12) with a calving margin width that widens gradually from ~65–90 km. While the widening calving margin may have acted to increase calving and thus exacerbate retreat, the decreasing trough depth (i.e., normal bed slope) could have acted to stabilize the ice margin (cf. Jones et al., 2015) although we note that the changes in depth are small compared to those encountered by contemporary ice streams in Antarctica. Given that these factors would counteract each other, and given that the changes are gradual and relatively small, we suggest that this trough geometry is not conducive to the very rapid retreat (*Stage 3*) implied by our modeled boundary ages. Additionally, this deglaciation continues during the relatively cooler conditions of Greenland Stadial 2 (GS-2) (Fig. 13). Given that neither trough geometry nor climate forcing can be directly correlated with the rapid nature of the observed retreat we infer that it is the result of ice sheet reorganization (drawdown) due to increased flux of ice to a stabilized grounding line, causing upstream thinning. The mass loss required to initiate the rapid retreat may well have been exacerbated by external forcing (i.e., GI-2) with increased calving due to warmer ocean waters as indicated by numerous records from ocean cores proximal to the former ISIS (Scourse et al., 2009). In this way the rapid retreat could be interpreted as a delayed response to climate forcing. The modeled rates of ice marginal retreat slow during *Stage 4* (*Wicklow–Howth*) and coincide with morphostratigraphic evidence for stillstands or marginal oscillation (McCabe and Ó Cofaigh, 1995; Rijsdijk et al., 2010). This period of slower retreat occurs across a reverse bedslope (Fig. 12). This seems counterintuitive as this scenario is widely cited as driving rapid grounding line retreat (e.g., Favier et al., 2014; Jamieson et al., 2012; Schoof, 2007), but again we note that the magnitude of depth change is small (<50 m). The more substantial accumulations of ice marginal sediment are both associated with bedrock highs on the lateral margin of the ice stream that may have acted as pinning points (McCabe, 2008), and could account for the slowing of the retreat rates observed during *Stage 4*. A similar scenario has been proposed for the Llŷn Peninsula, Wales, UK, on the opposite lateral margin of the ISIS (Smedley et al., 2017b).

CONCLUSIONS

The geochronological data presented here allow us to test a conceptual model of ISIS deglaciation in south and east Ireland inferred from the sediment-landform assemblage record. Integration of new geochronological data using Bayesian age modeling produces a conformable age model that supports the conceptual model of deglaciation, with extremely rapid (300–600 m a^{-1}) retreat from maximum extent, a slowing of retreat (26 m a^{-1}) during the period 25.9–24.2 ka, ice margin stabilization (3 m a^{-1}; 24.2–22.1 ka), rapid retreat (152 m a^{-1}; 22.1–21.6 ka), and finally a return to slower retreat rates (21 m a^{-1}; 21.6–19.5 ka).

This timescale strongly suggests that aspects of ISIS behavior during deglaciation displayed a complex relationship to external climatic forcing. Extremely rapid advance of the ISIS to its maximum extent, and its subsequent retreat at 26–25 ka is not directly correlated with distinct climate forcing in the North Atlantic region. Such behavior may be explained as a dynamic instability in response to overextension of the ice stream to the maximum limit that rendered it vulnerable to rapid retreat. Similarly, the stabilization of the ice margin at the Screen Hills spans a time of distinct warming (GI-2) with the subsequent rapid retreat occurring during colder conditions of GS-2. The stabilization at the Screen Hills is the most distinct change in pace of ISIS retreat evidenced by the data presented here and it occurs where there is a step-change in the confining trough geometry highlighting the important role that this plays in conditioning ice margin retreat. However, contrary to this, the ISIS subsequently underwent rapid retreat without major changes in trough geometry. We speculate that this represents a delayed response of the ice margin to the climate forcing of GI-2. Overall, changing trough geometry and internal feedbacks related to the overextension, retreat, and stabilization of the ISIS appear to obscure the role of external drivers such as climatic forcing.

The conceptual model and geochronological data presented here provide evidence for specific ice margin behavior during overall deglaciation that provides a testing ground for numerical models that likely require high resolution representations of grounding line dynamics. As contemporary ice streams in Greenland and Antarctica evolve in response to anthropogenic climate change they will undergo retreat that is conditioned both by climatic forcing and their internal dynamics. Our data highlight the potential for the evolution of rapid ice margin retreat to be highly nonlinear and conditioned strongly by trough geometry.

ACKNOWLEDGMENTS

This work was supported by the Natural Environment Research Council (NERC) consortium grant; BRITICE-CHRONO NE/J009768/1 (NE/J007196/1 to Durham University). The cosmogenic analyses were supported by the NERC Cosmogenic Isotope Analysis Facility allocation 9155.1014. Thanks are due to the staff at the Scottish Universities Environmental Research Centre accelerator mass spectrometry (SUERC AMS) Laboratory, East Kilbride, UK, for ^{10}Be isotope measurements. H. Wynne is thanked for etching the quartz grains for luminescence dating. We would like to thank the two reviewers, Jon Merritt and Benjamin Laabs, for constructive reviews that have improved this manuscript. Data used in this work is available from the author on reasonable request.

REFERENCES CITED

Arbic, B.K., Mitrovica, J.X., MacAyeal, D.R., and Milne, G.A., 2008, On the factors behind large Labrador Sea tides during the last glacial cycle and the potential implications for Heinrich events: Paleoceanography, v. 23, PA3211, https://doi.org/10.1029/2007PA001573.

Balco, G., Stone, J.O., Lifton, N.A., and Dunai, T.J., 2008, A complete and easily accessible means of calculating surface exposure ages or erosion rates from 10 Be and 26 Al measurements: Quaternary Geochronology, v. 3, p. 174–195, https://doi.org/10.1016/j.quageo.2007.12.001.

Bard, E., 2002, Climate shock: Abrupt changes over millennial time scales: Physics Today, v. 55, p. 32–38, https://doi.org/10.1063/1.1537910.

Bard, E., Rostek, F., and Menot-Combes, G., 2004, A better radiocarbon clock: Science, v. 303, p. 178–179, https://doi.org/10.1126/science.1091964.

Benn, D.I., Warren, C.R., and Mottram, R.H., 2007, Calving processes and the dynamics of calving glaciers: Earth-Science Reviews, v. 82, p. 143–179, https://doi.org/10.1016/j.earscirev.2007.02.002.

Bennett, M.R., 2003, Ice streams as the arteries of an ice sheet: Their mechanics, stability and significance: Earth-Science Reviews, v. 61, p. 309–339, https://doi.org/10.1016/S0012-8252(02)00130-7.

Bintanja, R., van de Wal, R.S.W., and Oerlemans, J., 2005, Modelled atmospheric temperatures and global sea levels over the past million years: Nature, v. 437, p. 125–128, https://doi.org/10.1038/nature03975.

Borchers, B., Marrero, S., Balco, G., Caffee, M., Goehring, B., Lifton, N., Nishiizumi, K., Phillips, F., Schaefer,

J., and Stone, J., 2016, Geological calibration of spallation production rates in the CRONUS-Earth project: Quaternary Geochronology, v. 31, p. 188–198, https://doi.org/10.1016/j.quageo.2015.01.009.

Bøtter-Jensen, L., Andersen, C.E., Duller, G.A.T., and Murray, A.S., 2003, Developments in radiation, stimulation and observation facilities in luminescence measurements: Radiation Measurements, v. 37, p. 535–541, https://doi.org/10.1016/S1350-4487(03)00020-9.

Bradley, S.L., Milne, G.A., Shennan, I., and Edwards, R., 2011, An improved glacial isostatic adjustment model for the British Isles: Journal of Quaternary Science, v. 26, p. 541–552, https://doi.org/10.1002/jqs.1481.

Briner, J.P., and Swanson, T.W., 1998, Using inherited cosmogenic 36Cl to constrain glacial erosion rates of the Cordilleran ice sheet: Geology, v. 26, p. 3–6, https://doi.org/10.1130/0091-7613(1998)026<0003:UICCTC>2.3.CO;2.

Bromley, G.R., Putnam, A.E., Rademaker, K.M., Lowell, T.V., Schaefer, J.M., Hall, B., Winckler, G., Birkel, S.D., and Borns, H.W., 2014, Younger Dryas deglaciation of Scotland driven by warming summers: Proceedings of the National Academy of Sciences of the United States of America, v. 111, p. 6215–6219, https://doi.org/10.1073/pnas.1321122111.

Bronk Ramsey, C., 2009, Dealing with outliers and offsets in radiocarbon dating: Radiocarbon, v. 51, p. 1023–1045, https://doi.org/10.1017/S0033822200034093.

Bronk Ramsey, C., 2017, OxCal 4.3.2, http://c14.arch.ox.ac.uk/oxcalhelp/hlp_contents.html (accessed February 2018).

Buck, C.E., Kenworthy, J.B., Litton, C.D., and Smith, A.F.M., 1991, Combining archaeological and radiocarbon information: A Bayesian approach to calibration: Antiquity, v. 65, p. 808–821, https://doi.org/10.1017/S0003598X00080534.

Child, D., Elliott, G., Mifsud, C., Smith, A.M., and Fink, D., 2000, Sample processing for earth science studies at ANTARES: Nuclear Instruments & Methods in Physics Research. Section B, Beam Interactions with Materials and Atoms, v. 172, p. 856–860, https://doi.org/10.1016/S0168-583X(00)00198-1.

Chiverrell, R.C., Thrasher, I.M., Thomas, G.S.P., Lang, A., Scourse, J.D., van Landeghem, K.J.J., McCarroll, D., Clark, C.D., Ó Cofaigh, C., Evans, D.J.A., and Ballantyne, C.K., 2013, Bayesian modelling the retreat of the Irish Sea Ice Stream: Journal of Quaternary Science, v. 28, p. 200–209, https://doi.org/10.1002/jqs.2616.

Clark, J., McCabe, A.M., Bowen, D.Q., and Clark, P.U., 2012, Response of the Irish Ice Sheet to abrupt climate change during the last deglaciation: Quaternary Science Reviews, v. 35, p. 100–115, https://doi.org/10.1016/j.quascirev.2012.01.001.

Colgan, P.M., Bierman, P.R., Mickelson, D.M., and Caffee, M., 2002, Variation in glacial erosion near the southern margin of the Laurentide Ice Sheet, south-central Wisconsin, USA: Implications for cosmogenic dating of glacial terrains: Geological Society of America Bulletin, v. 114, p. 1581–1591, https://doi.org/10.1130/0016-7606(2002)114<1581:VIGENT>2.0.CO;2.

Duller, G.A.T., 2008, Single grain optical dating of Quaternary sediments: Why aliquot size matters in luminescence dating: Boreas, v. 37, p. 589–612, https://doi.org/10.1111/j.1502-3885.2008.00051.x.

Durcan, J.A., King, G.E., and Duller, G.A.T., 2015, DRAC: Dose Rate and Age Calculator for trapped charge dating: Quaternary Geochronology, v. 28, p. 54–61, https://doi.org/10.1016/j.quageo.2015.03.012.

Evans, D.J.A., and Ó Cofaigh, C., 2003, Depositional evidence for marginal oscillations of the Irish Sea ice stream in southeast Ireland during the last glaciation: Boreas, v. 32, p. 76–101, 10.1111/j.1502-3885.2003.tb01443.x.

Eyles, N., and McCabe, A.M., 1989, The Late Devensian (<22,000 BP) Irish Sea Basin: The sedimentary record of a collapsed ice sheet margin: Quaternary Science Reviews, v. 8, p. 307–351, https://doi.org/10.1016/0277-3791(89)90034-6.

Fabel, D., Ballantyne, C.K., and Xu, S., 2012, Trimlines, blockfields, mountain-top erratics and the vertical dimensions of the last British–Irish Ice Sheet in NW Scotland: Quaternary Science Reviews, v. 55, p. 91–102, https://doi.org/10.1016/j.quascirev.2012.09.002.

Favier, L., Durand, G., Cornford, S.L., Gudmundsson, G.H., Gagliardini, O., Gillet-Chaulet, F., Zwinger, T., Payne, A.J., and Le Brocq, A.M., 2014, Retreat of Pine Island Glacier controlled by marine ice-sheet instability: Nature Climate Change, v. 4, no. 2, p. 117, https://doi.org/10.1038/nclimate2094.

Galbraith, R.F., and Laslett, G.M., 1993, Statistical models for mixed fission track ages: Nuclear Tracks and Radiation Measurements, v. 21, p. 459–470, https://doi.org/10.1016/1359-0189(93)90185-C.

Galbraith, R.F., Roberts, R.G., Laslett, G.M., Yoshida, H., and Olley, J.M., 1999, Optical dating of single and multiple grains of quartz from jinmium rock shelter, northern Australia: Part i, experimental design and statistical models: Archaeometry, v. 41, p. 339–364, https://doi.org/10.1111/j.1475-4754.1999.tb00987.x.

Guérin, G., Mercier, N., and Adamiec, G., 2011, Dose-rate conversion factors: Update: Ancient TL, v. 29, p. 5–8.

Guérin, G., Mercier, N., Nathan, R., Adamiec, G., and Lefrais, Y., 2012, On the use of the infinite matrix assumption and associated concepts: A critical review: Radiation Measurements, v. 47, no. 9, p. 778–785, https://doi.org/10.1016/j.radmeas.2012.04.004.

Haapaniemi, A.I., Scourse, J.D., Peck, V.L., Kennedy, H., Kennedy, P., Hemming, S.R., Furze, M.F., Pieńkowski, A.J., Austin, W.E., Walden, J., and Wadsworth, E., 2010, Source, timing, frequency and flux of ice-rafted detritus to the Northeast Atlantic margin, 30–12 ka: Testing the Heinrich precursor hypothesis: Boreas, v. 39, p. 576–591.

Heyman, J., Stroeven, A.P., Harbor, J.M., and Caffee, M.W., 2011, Too young or too old: Evaluating cosmogenic exposure dating based on an analysis of compiled boulder exposure ages: Earth and Planetary Science Letters, v. 302, p. 71–80, https://doi.org/10.1016/j.epsl.2010.11.040.

Hiemstra, J.F., Evans, D.J., Scourse, J.D., McCarroll, D., Furze, M.F., and Rhodes, E., 2006, New evidence for a grounded Irish Sea glaciation of the Isles of Scilly, UK: Quaternary Science Reviews, v. 25, p. 299–309, https://doi.org/10.1016/j.quascirev.2005.01.013.

Jamieson, S.S., Vieli, A., Livingstone, S.J., Ó Cofaigh, C., Stokes, C., Hillenbrand, C.D., and Dowdeswell, J.A., 2012, Ice-stream stability on a reverse bed slope: Nature Geoscience, v. 5, p. 799–802, https://doi.org/10.1038/ngeo1600.

Jones, R.S., Mackintosh, A.N., Norton, K.P., Golledge, N.R., Fogwill, C.J., Kubik, P.W., Christl, M., and Greenwood, S.L., 2015, Rapid Holocene thinning of an East Antarctic outlet glacier driven by marine ice sheet instability: Nature Communications, v. 6, p. 8910, https://doi.org/10.1038/ncomms9910.

Joughin, I., and Alley, R.B., 2011, Stability of the West Antarctic ice sheet in a warming world: Nature Geoscience, v. 4, p. 506–513, https://doi.org/10.1038/ngeo1194.

Joughin, I., Smith, B.E., and Medley, B., 2014, Marine ice sheet collapse potentially under way for the Thwaites Glacier Basin, West Antarctica: Science, v. 344, p. 735–738, https://doi.org/10.1126/science.1249055.

Kohl, C.P., and Nishiizumi, K., 1992, Chemical isolation of quartz for measurement of in-situ-produced cosmogenic nuclides: Geochimica et Cosmochimica Acta, v. 56, p. 3583–3587, https://doi.org/10.1016/0016-7037(92)90401-4.

Lal, D., 1991, Cosmic ray labeling of erosion surfaces: In situ nuclide production rates and erosion models: Earth and Planetary Science Letters, v. 104, p. 424–439, https://doi.org/10.1016/0012-821X(91)90220-C.

Lambeck, K., and Purcell, A.P., 2001, Sea-level change in the Irish Sea since the Last Glacial Maximum: Constraints from isostatic modelling: Journal of Quaternary Science, v. 16, p. 497–506, https://doi.org/10.1002/jqs.638.

Lamplugh, G.W., 1903. The Geology of the Country Around Dublin: (Explanation of Sheet 112). HM Stationery Office, Dublin, Ireland, 166 p.

Lawrence, K.T., Herbert, T.D., Brown, C.M., Raymo, M.E., and Haywood, A.M., 2009, High-amplitude variations in North Atlantic sea surface temperature during the early Pliocene warm period: Paleoceanography, v. 24, PA2218, https://doi.org/10.1029/2008PA001669.

Lifton, N., Sato, T., and Dunai, T.J., 2014, Scaling in situ cosmogenic nuclide production rates using analytical approximations to atmospheric cosmic-ray fluxes: Earth and Planetary Science Letters, v. 386, p. 149–160, https://doi.org/10.1016/j.epsl.2013.10.052.

Ma, Y., Tripathy, C.S., and Bassis, J.N., 2017, Bounds on the calving cliff height of marine terminating glaciers: Geophysical Research Letters, v. 44, https://doi.org/10.1002/2016GL071560.

Martin, L.C.P., Blard, P.H., Balco, G., Lavé, J., Delunel, R., Lifton, N., and Laurent, V., 2017, The CREp program and the ICE-D production rate calibration database: A fully parameterizable and updated online tool to compute cosmic-ray exposure ages: Quaternary Geochronology, v. 38, p. 25–49, https://doi.org/10.1016/j.quageo.2016.11.006.

Marrero, S.M., Phillips, F.M., Borchers, B., Lifton, N., Aumer, R., and Balco, G., 2016, Cosmogenic nuclide systematics and the CRONUScalc program: Quaternary Geochronology, v. 31, p. 160–187, https://doi.org/10.1016/j.quageo.2015.09.005.

McCabe, A.M., 1997, Geological constraints on geophysical models of relative sea-level change during deglaciation of the western Irish Sea basin: Journal of the Geological Society, v. 154, p. 601–604, https://doi.org/10.1144/gsjgs.154.4.0601.

McCabe, A.M., 2008. Glacial geology and geomorphology: The landscapes of Ireland. Dunedin Academic Press Ltd., Edinburgh, UK, 274 p.

McCabe, A., and Ó Cofaigh, C., 1995, Late Pleistocene morainal bank facies at Greystones, eastern Ireland: An example of sedimentation during ice marginal re-equilibration in an isostatically depressed basin: Sedimentology, v. 42, p. 647–663, https://doi.org/10.1111/j.1365-3091.1995.tb00398.x.

Mosola, A.B., and Anderson, J.B., 2006, Expansion and rapid retreat of the West Antarctic Ice Sheet in eastern Ross Sea: Possible consequence of over-extended ice streams?: Quaternary Science Reviews, v. 25, p. 2177–2196, https://doi.org/10.1016/j.quascirev.2005.12.013.

Ó Cofaigh, C., and Evans, D.J., 2001a, Deforming bed conditions associated with a major ice stream of the last British ice sheet: Geology, v. 29, p. 795–798, 10.1130/0091-7613(2001)029<0795:DBCAWA>2.0.CO;2.

Ó Cofaigh, C., and Evans, D.J.A., 2001b, Sedimentary evidence for deforming bed conditions associated with a grounded Irish Sea glacier, southern Ireland: Journal of Quaternary Science, v. 16, p. 435–454, 10.1002/jqs.631.

Ó Cofaigh, C., and Evans, D.J.A., 2007, Radiocarbon constraints on the age of the maximum advance of the British–Irish Ice Sheet in the Celtic Sea: Quaternary Science Reviews, v. 26, p. 1197–1203, 10.1016/j.quascirev.2007.03.008.

Ó Cofaigh, C., Telfer, M.W., Bailey, R.M., and Evans, D.J., 2012, Late Pleistocene chronostratigraphy and ice sheet limits, southern Ireland: Quaternary Science Reviews, v. 44, p. 160–179, https://doi.org/10.1016/j.quascirev.2010.01.011.

O'Connor, P.J., Kennan, P.S., and Aftalion, M., 1988, New Rb–Sr and U–Pb ages for the Carnsore Granite and their bearing on the antiquity of the Rosslare Complex, southeastern Ireland: Geological Magazine, v. 125, p. 25–29, https://doi.org/10.1017/S0016756800009341.

Payne, A.J., Vieli, A., Shepherd, A.P., Wingham, D.J., and Rignot, E., 2004, Recent dramatic thinning of largest West Antarctic ice stream triggered by oceans: Geophysical Research Letters, v. 31, p. L23401, https://doi.org/10.1029/2004GL021284.

Phillips, F.M., Argento, D.C., Balco, G., Caffee, M.W., Clem, J., Dunai, T.J., Finkel, R., Goehring, B., Gosse, J.C., Hudson, A.M., and Jull, A.T., 2016, The CRONUS-Earth project: a synthesis: Quaternary Geochronology, v. 31, p. 119–154, https://doi.org/10.1016/j.quageo.2015.09.006.

Pollard, D., DeConto, R.M., and Alley, R.B., 2015, Potential Antarctic Ice Sheet retreat driven by hydrofracturing and ice cliff failure: Earth and Planetary Science Let-

ters, v. 412, p. 112–121, https://doi.org/10.1016/j.epsl.2014.12.035.

Praeg, D., McCarron, S., Dove, D., Ó Cofaigh, C., Scott, G., Monteys, X., Facchin, L., Romeo, R., and Coxon, P., 2015, Ice sheet extension to the Celtic Sea shelf edge at the Last Glacial Maximum: Quaternary Science Reviews, v. 111, p. 107–112, https://doi.org/10.1016/j.quascirev.2014.12.010.

Prescott, J.R., and Hutton, J.T., 1994, Cosmic-Ray Contributions to Dose-Rates for Luminescence and ESR Dating—Large Depths and Long-Term Time Variations: Radiation Measurements, v. 23, no. 2-3, p. 497–500, https://doi.org/10.1016/1350-4487(94)90086-8.

Putkonen, J., and Swanson, T., 2003, Accuracy of cosmogenic ages for moraines: Quaternary Research, v. 59, p. 255–261, https://doi.org/10.1016/S0033-5894(03)00006-1.

Putnam, A.E., Schaefer, J.M., Barrell, D.J.A., Vandergoes, M., Denton, G.H., Kaplan, M.R., Finkel, R.C., Schwartz, R., Goehring, B.M., and Kelley, S.E., 2010, In situ cosmogenic ^{10}Be production-rate calibration from the Southern Alps, New Zealand: Quaternary Geochronology, v. 5, no. 4, p. 392–409, https://doi.org/10.1016/j.quageo.2009.12.001.

Rasmussen, S.O., Bigler, M., Blockley, S.P., Blunier, T., Buchardt, S.L., Clausen, H.B., Cvijanovic, I., Dahl-Jensen, D., Johnsen, S.J., Fischer, H., and Gkinis, V., 2014, A stratigraphic framework for abrupt climatic changes during the Last Glacial period based on three synchronized Greenland ice-core records: Refining and extending the INTIMATE event stratigraphy: Quaternary Science Reviews, v. 106, p. 14–28, https://doi.org/10.1016/j.quascirev.2014.09.007.

Ravier, E., Buoncristiani, J.F., Clerc, S., Guiraud, M., Menzies, J., and Portier, E., 2014, Sedimentological and deformational criteria for discriminating subglacifluvial deposits from subaqueous ice-contact fan deposits: A Pleistocene example (Ireland): Sedimentology, v. 61, p. 1382–1410, https://doi.org/10.1111/sed.12111.

Rijsdijk, K.F., Warren, W.P., and van der Meer, J.J., 2010, The glacial sequence at Killiney, SE Ireland: Terrestrial deglaciation and polyphase glacitectonic deformation: Quaternary Science Reviews, v. 29, p. 696–719, https://doi.org/10.1016/j.quascirev.2009.11.011.

Rignot, E., Mouginot, J., Morlighem, M., Seroussi, H., and Scheuchl, B., 2014, Widespread, rapid grounding line retreat of Pine Island, Thwaites, Smith, and Kohler glaciers, West Antarctica, from 1992 to 2011: Geophysical Research Letters, v. 41, p. 3502–3509, https://doi.org/10.1002/2014GL060140.

Roberts, D.H., Dackombe, R.V., and Thomas, G.S., 2007, Palaeo-ice streaming in the central sector of the British—Irish Ice Sheet during the Last Glacial Maximum: Evidence from the northern Irish Sea Basin: Boreas, v. 36, p. 115–129, https://doi.org/10.1111/j.1502-3885.2007.tb01186.x.

Schoof, C., 2007, Ice sheet grounding line dynamics: Steady states, stability, and hysteresis: Journal of Geophysical Research. Earth Surface, v. 112, p. F03S28.

Scourse, J.D., and Furze, M.F.A., 2001, A critical review of the glaciomarine model for Irish Sea deglaciation: Evidence from southern Britain, the Celtic shelf and adjacent continental slope: Journal of Quaternary Science, v. 16, p. 419–434, https://doi.org/10.1002/jqs.629.

Scourse, J.D., Austin, W.E.N., Bateman, R.M., Catt, J.A., Evans, C.D.R., Robinson, J.E., and Young, J.R., 1990, Sedimentology and micropalaeontology of glacimarine sediments from the central and southwestern Celtic Sea, *in* Dowdeswell, J.A., and Scourse, J.D., eds., Glacimarine Environments: Processes and Sediments: Geological Society of London, Special Publication 53, p. 329–347, https://doi.org/10.1144/GSL.SP.1990.053.01.19.

Scourse, J.D., Haapaniemi, A.I., Colmenero-Hidalgo, E., Peck, V.L., Hall, I.R., Austin, W.E., Knutz, P.C., and Zahn, R., 2009, Growth, dynamics and deglaciation of the last British–Irish ice sheet: The deep-sea ice-rafted detritus record: Quaternary Science Reviews, v. 28, p. 3066–3084, https://doi.org/10.1016/j.quascirev.2009.08.009.

Scourse, J.D., Ward, S.L., Wainwright, A., Uehara, K., and Bradley, S., 2018, The role of megatides and relative sea level in controlling the deglaciation of the British-Irish and Fennoscandian Ice Sheets: Journal of Quaternary Science, v. 33, p. 139–149, https://doi.org/10.1002/jqs.3011.

Seierstad, I.K., Abbott, P.M., Bigler, M., Blunier, T., Bourne, A.J., Brook, E., Buchardt, S.L., Buizert, C., Clausen, H.B., Cook, E., and Dahl-Jensen, D., 2014, Consistently dated records from the Greenland GRIP, GISP2 and NGRIP ice cores for the past 104 ka reveal regional millennial-scale δ^{18}O gradients with possible Heinrich event imprint: Quaternary Science Reviews, v. 106, p. 29–46, https://doi.org/10.1016/j.quascirev.2014.10.032.

Small, D., and Fabel, D., 2015, A Lateglacial ^{10}Be production rate from glacial lake shorelines in Scotland: Journal of Quaternary Science, v. 30, p. 509–513, https://doi.org/10.1002/jqs.2804.

Small, D., and Fabel, D., 2016a, Response to Bromley et al. "Comment on 'Was Scotland deglaciated during the Younger Dryas?' By Small and Fabel (2016)": Quaternary Science Reviews, v. 152, p. 206–208, https://doi.org/10.1016/j.quascirev.2016.09.021.

Small, D., and Fabel, D., 2016b, Was Scotland deglaciated during the Younger Dryas?: Quaternary Science Reviews, v. 145, p. 259–263, https://doi.org/10.1016/j.quascirev.2016.05.031.

Small, D., Clark, C.D., Chiverrell, R.C., Smedley, R.K., Bateman, M.D., Duller, G.A., Ely, J.C., Fabel, D., Medialdea, A., and Moreton, S.G., 2017, Devising quality assurance procedures for assessment of legacy geochronological data relating to deglaciation of the last British-Irish Ice Sheet: Earth-Science Reviews, v. 164, p. 232–250, https://doi.org/10.1016/j.earscirev.2016.11.007.

Smedley, R.K., Scourse, J.D., Small, D., Hiemstra, J.F., Duller, G.A.T., Bateman, M.D., Burke, M.J., Chiverrell, R.C., Clark, C.D., Davies, S.M., Fabel, D., Gheorghiu, D.M., McCarroll, D., Medialdea, A., and Xu, S., 2017a, New age constraints for the limit of the British-Irish Ice Sheet on the Isles of Scilly: Journal of Quaternary Science, v. 32, p. 48–62, https://doi.org/10.1002/jqs.2922.

Smedley, R.K., Chiverrell, R.C., Ballantyne, C.K., Burke, M.J., Clark, C.D., Duller, G.A.T., Fabel, D., McCarroll, D., Scourse, J.D., Small, D., and Thomas, G.S.P., 2017b, Internal dynamics condition centennial-scale oscillations in marine-based ice stream retreat: Geology, v. 45, p. 787–790, https://doi.org/10.1130/G38991.1.

Stephens, N., and Synge, F.M., 1957, January. A Quaternary succession at Sutton, co. Dublin, *in* Proceedings of the Royal Irish Academy, Section B: Biological, Geological, and Chemical Science: Hodges, Figgis, & Co., p. 19–27.

Stone, J.O., 2000, Air pressure and cosmogenic isotope production: Journal of Geophysical Research. Solid Earth, v. 105, p. 23753–23759, https://doi.org/10.1029/2000JB900181.

Stokes, C.R., and Clark, C.D., 2001, Palaeo-ice streams: Quaternary Science Reviews, v. 20, p. 1437–1457, https://doi.org/10.1016/S0277-3791(01)00003-8.

Stokes, C.R., Tarasov, L., Blomdin, R., Cronin, T.M., Fisher, T.G., Gyllencreutz, R., Hättestrand, C., Heyman, J., Hindmarsh, R.C., Hughes, A.L., and Jakobsson, M., 2015, On the reconstruction of palaeo-ice sheets: Recent advances and future challenges: Quaternary Science Reviews, v. 125, p. 15–49, https://doi.org/10.1016/j.quascirev.2015.07.016.

Stokes, C.R., Margold, M., Clark, C.D., and Tarasov, L., 2016, Ice stream activity scaled to ice sheet volume during Laurentide Ice Sheet deglaciation: Nature, v. 530, p. 322–326, https://doi.org/10.1038/nature16947.

Thomas, G.S.P., and Chiverrell, R.C., 2011, Styles of structural deformation and syn-tectonic sedimentation around the margins of the late Devensian Irish Sea Ice Stream: The Isle of Man, Llyn Peninsula and County Wexford: Glacitectonics: A Field Guide, Quaternary Research Association, p. 59–78.

Thomas, G.S.P., and Kerr, P., 1987, The stratigraphy, sedimentology and palaeontology of the Pleistocene Knocknasilloge Member, Co. Wexford. Ireland: Geological Journal, v. 22, p. 67–82, https://doi.org/10.1002/gj.3350220202.

Thomas, G.S.P., and Summers, A.J., 1983, The quaternary stratigraphy between Blackwater harbour and Tinnaberna, county Wexford: Journal of Earth Sciences Royal Dublin Society, v. 5, p. 121–134.

Thomas, G.S.P., and Summers, A., 1984, Glacio-dynamic structures from the Blackwater Formation, Co. Wexford, Ireland: Boreas, v. 13, p. 5–12, https://doi.org/10.1111/j.1502-3885.1984.tb00053.x.

Van Landeghem, K.J., Wheeler, A.J., and Mitchell, N.C., 2009, Seafloor evidence for palaeo-ice streaming and calving of the grounded Irish Sea Ice Stream: Implications for the interpretation of its final deglaciation phase: Boreas, v. 38, p. 119–131, https://doi.org/10.1111/j.1502-3885.2008.00041.x.

Xu, S., Dougans, A.B., Freeman, S.P., Schnabel, C., and Wilcken, K.M., 2010, Improved 10 Be and 26 Al-AMS with a 5MV spectrometer: Nuclear Instruments & Methods in Physics Research. Section B, Beam Interactions with Materials and Atoms, v. 268, p. 736–738, https://doi.org/10.1016/j.nimb.2009.10.018.

Young, N.E., Schaefer, J.M., Briner, J.P., and Goehring, B.M., 2013, A ^{10}Be production-rate calibration for the Arctic: Journal of Quaternary Science, v. 28, no. 5, p. 515–526, https://doi.org/10.1002/jqs.2642.

Science Editor: Bradley S. Singer
Associate Editor: Benjamin Laabs

Manuscript Received 30 May 2017
Revised Manuscript Received 1 March 2018
Manuscript Accepted 16 April 2018

Printed in the USA